Eur. Phys. J. B **13**, 55–73 (2000)

THE EUROPEAN PHYSICAL JOURNAL B

EDP Sciences

Magnetic properties of zig-zag ladders*

D.C. Cabra[1,a], A. Honecker[2,3,b,c], and P. Pujol[4]

[1] Physikalisches Institut der Universität Bonn, Nußallee 12, 53115 Bonn, Germany
[2] International School for Advanced Studies, Via Beirut 2-4, 34014 Trieste, Italy
[3] Institut für Theoretische Physik, ETH-Hönggerberg, 8093 Zürich, Switzerland
[4] Laboratoire de Physique[d], Groupe de Physique Théorique, ENS Lyon, 46 Allée d'Italie, 69364 Lyon Cedex 07, France

Received 11 February 1999 and Received in final form 16 June 1999

Abstract. We analyze the phase diagram of a system of spin-1/2 Heisenberg antiferromagnetic chains interacting through a zig-zag coupling, also called zig-zag ladders. Using bosonization techniques we study how a spin-gap or more generally plateaux in magnetization curves arise in different situations. While for coupled XXZ chains, one has to deal with a recently discovered chiral perturbation, the coupling term which is present for normal ladders is restored by an external magnetic field, dimerization or the presence of charge carriers. We then proceed with a numerical investigation of the phase diagram of two coupled Heisenberg chains in the presence of a magnetic field. Unusual behaviour is found for ferromagnetic coupled antiferromagnetic chains. Finally, for three (and more) legs one can choose different inequivalent types of coupling between the chains. We find that the three-leg ladder can exhibit a spin-gap and/or non-trivial plateaux in the magnetization curve whose appearance strongly depends on the choice of coupling.

PACS. 75.10.Jm Quantized spin models – 75.40.Cx Static properties (order parameter, static susceptibility, heat capacities, critical exponents, etc.) – 75.45.+j Macroscopic quantum phenomena in magnetic systems

1 Introduction

In the last few years, the study of quasi-one dimensional magnets has become intense. One of the main reasons is the appearance of real materials which can be well approximated by one-dimensional models. An important class corresponds to the so-called spin ladder materials, such as the compounds $Sr_{x-1}Cu_xO_{2x-1}$ and $La_{4+4x}Cu_{8+2x}O_{14+8x}$ which are closely related to high-T_c compounds (for reviews see *e.g.* [1,2]) or the organic two-leg ladder material $Cu_2(C_5H_{12}N_2)_2Cl_4$ (see *e.g.* [3]).

In addition, the similarities in the normal-state properties of high-temperature superconductors and ladder cuprates make these latter systems valuable laboratories from both the theoretical and experimental point of view.

Due to the low dimensionality, quantum fluctuations are crucial and because of this, these systems exhibit a variety of interesting phenomena such as the appearance of plateaux in magnetization curves, an issue that has received a lot of attention recently (see *e.g.* [4–20]).

The study of spin ladder systems with different topologies of couplings has been also motivated both from the experimental and the theoretical side. In particular, the zig-zag coupling between quantum spin chains has received much theoretical attention [21–25]. In the case of antiferromagnetic (AF) couplings, the zig-zag array introduces frustration which makes the study of these systems much more difficult. Apart from being a possible approach to study the two-dimensional triangular lattice, this topology of couplings is realized in a number of quasi-one dimensional compounds, such as Cs_2CuCl_4 [26], $KCuCl_3$ and $TlCuCl_3$ [27] as well as NH_4CuCl_3 [28]. A (two-dimensional) zig-zag arrangement is also present in $SrCuO_2$. At room temperature, the materials $KCuCl_3$, $TlCuCl_3$ and NH_4CuCl_3 are isostructural and can be described by an alternating two-leg zig-zag ladder [27,28]. Experimentally, one observes a zero magnetization plateau in the low-temperature magnetization process of $KCuCl_3$ and $TlCuCl_3$ [27], whereas for NH_4CuCl_3 plateaux in the magnetization curve are observed at 1/4 and 3/4 of the saturation magnetization [28]. While the former is in good agreement with the theoretical predictions (which will be

* Work done under partial support of the EC TMR Programme *Integrability, non-perturbative effects and symmetry in Quantum Field Theories*, grant FMRX-CT96-0012.

[a] On leave of absence from the Universidad Nacional de La Plata and Universidad Nacional de Lomas de Zamora, Argentina
[b] A Feodor-Lynen fellow of the Alexander von Humboldt-foundation, e-mail: a.honecker@tu-bs.de
[c] *Present address*: Institut für Theoretische Physik, TU Braunschweig, 38106 Braunschweig, Germany
[d] URA 1325 du CNRS associée à l'École Normale Supérieure de Lyon

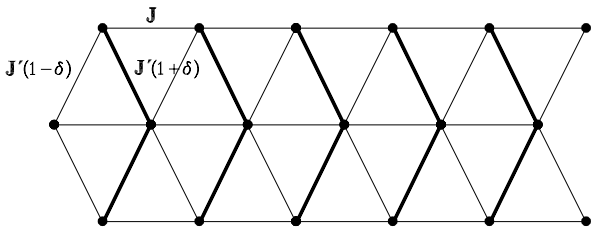

Fig. 1. Generic structure of the ladders considered in the present paper.

discussed in detail in this paper), the explanation of the latter is still unclear (even though explanations have already been proposed [29]). A detailed analysis of related structures such as those studied in the present paper can be expected to be also useful for interpreting these experiments.

Zig-zag coupled chains also have several special properties which render them an interesting problem from a purely theoretical point of view. Firstly, unlike many other systems they do not have a simple 'strong-coupling' limit where the system is decoupled into finite clusters of spins. If there is such a decoupling limit, the possible values of the magnetization are clearly quantized in this limit and using perturbation theory one can easily understand the appearance of magnetization plateaux in the strong-coupling region [10,13,15]. For example, for the usual spin ladders, one finds a quantization condition on the magnetization $\langle M\rangle$ (which we normalize to saturation value 1) for the appearance of a plateau in the magnetization curve [10,13] (compare also [6,9,14,15,18]):

$$SV(1-\langle M\rangle)\in\mathbb{Z}. \tag{1.1}$$

Here S is the spin on each site and V is the volume of a translationally invariant unit cell. For N-leg ladders, $V = lN$ where l is the period of explicit or spontaneous breaking of translational symmetry in the magnetized groundstate.

Since zig-zag coupled chains with no or weak dimerization do not have a simple strong-coupling limit, it is not immediately clear if the condition for the appearance of plateaux in zig-zag ladders will also be given by (1.1). The fact that the zig-zag coupling is frustrating is a further reason why the quantization condition on the magnetization or *e.g.* the universality classes of the transitions at the plateau boundaries might be different. From a field theoretical point of view, zig-zag coupling is also interesting because at zero field it cancels the most relevant coupling term for the usual ladders and instead one has to deal with a chirally asymmetric perturbation [24].

After mentioning all these possibilities for a different behaviour we should, however, immediately point out that one of our main conclusions is going to be that zig-zag coupling is not very different from the ordinary one. In particular, the most relevant interaction term is recovered in many situations like the presence of a magnetic field, dimerization or charge carriers. We will also find that all observed magnetization plateaux have a natural interpretation in terms of the quantization condition (1.1).

Motivation for studying these systems arises also from other fields. For example, spin ladders arise in the study of gated Josephson junction arrays [30]. Even more, reference [22] pointed out a close analogy between the two-leg zig-zag ladder and the doped Kondo lattice model. This model in turn is believed to be relevant to the phenomenon of colossal magnetoresistance in metallic oxides and has therefore received renewed attention recently [31].

The main focus of the present paper are N coupled Heisenberg chains with a dimerized zig-zag coupling (see also Fig. 1)

$$\begin{aligned} H^{(N)} = {} & J\sum_{i=1}^{N}\sum_{x=1}^{L}\mathbf{S}_{i,x}\cdot\mathbf{S}_{i,x+1} \\ & + J'\sum_{i=1}^{N}\sum_{x=1}^{L}\mathbf{S}_{i,x}\big((1+\delta)\,\mathbf{S}_{i+1,x}+(1-\delta)\,\mathbf{S}_{i+1,x+1}\big) \\ & - h\sum_{i,x}S^z_{i,x}. \end{aligned} \tag{1.2}$$

For compactness of presentation we have written scalar products here, but we will also consider the case where an XXZ anisotropy Δ is introduced in the obvious way. We will furthermore discuss a similar system including dimerization along the chains and also charge degrees of freedom, *i.e.* Hubbard zig-zag ladders. In equation (1.2) there is also some ambiguity in writing the interchain coupling, in particular in combination with specifying boundary conditions for $N > 2$ – an issue to which we shall return later.

The two-leg zig-zag ladder can be reinterpreted as a Heisenberg chain with next-nearest-neighbour interactions. In this interpretation, the study of this system has a long history going back at least to [32]. One intriguing observation regarding this system is that for special parameters the groundstate takes a very simple form and correlation functions can be computed exactly [33,34].

This paper is organized as follows: In Section 2 we examine the Hamiltonian (1.2) at $\delta = h = 0$ without and with XXZ anisotropy, using non-Abelian and Abelian bosonization, respectively. Section 3 is devoted to a field-theoretical analysis of the effect of various modifications: An external magnetic field, dimerization or doping with charge carriers. In Section 4 we then numerically investigate the magnetization process of the two-leg ladder (1.2) and discuss the various commensurate and incommensurate phases appearing for $J' > 0$ as well as $J' < 0$. In Section 5 we investigate the transition to saturation of the two-leg zig-zag ladder in some detail. Finally, in Section 6 we numerically compute magnetization curves for several variants of the three-leg zig-zag ladder. An appendix contains some supplementary material.

2 Field theory for zero magnetic field

2.1 The SU(2) symmetric case

First, we reexamine the simplest case of the $SU(2)$ symmetric two-leg zig-zag ladder that has been studied previously in [22,23].

We start by reviewing some of the earlier results. In the weak (interchain) coupling limit each of the chains can be described by the level 1 Wess-Zumino-Witten (WZW) model [35,36] with the action given by

$$W[g^i] = \frac{1}{8\pi}\int_{\mathbb{R}^2} \mathrm{d}^2x \mathrm{tr}(\partial_\mu g^i \partial^\mu g^{i^{-1}}) + \Gamma[g^i], \qquad (2.1)$$

where the superscript i labels the different chains, g^i takes values in the Lie group $SU(2)$ and $\Gamma[g]$ is the Wess-Zumino term

$$\Gamma[g] = \frac{1}{12\pi}\int_Y \mathrm{d}^3y \epsilon_{\alpha\beta\gamma}\mathrm{tr}(g^{-1}\partial_\alpha g g^{-1}\partial_\beta g g^{-1}\partial_\gamma g), \quad (2.2)$$

with Y a three-dimensional manifold having $\mathbb{R}^2$ as boundary.

The bosonized expression for the spin operator is given by

$$\mathbf{S}^i(x) = \mathbf{J}^i_{\mathrm{R}} + \mathbf{J}^i_{\mathrm{L}} + B(-1)^x \mathrm{tr}(\boldsymbol{\sigma} g^i) \qquad (2.3)$$

where

$$J^{i,a}_{\mathrm{R}} = -\frac{1}{2\pi}\mathrm{tr}\big((\partial_+ g^i)(g^i)^{-1}\sigma^a\big),$$
$$J^{i,a}_{\mathrm{L}} = \frac{1}{2\pi}\mathrm{tr}\big((g^i)^{-1}\partial_- g^i \sigma^a\big)$$

are the WZW currents satisfying a $\widehat{su(2)}_1$ Kac-Moody algebra and B is a non-universal constant.

The marginally irrelevant perturbation term

$$-\lambda\sum_i \int \mathrm{d}x \mathbf{J}^i_{\mathrm{R}}\cdot\mathbf{J}^i_{\mathrm{L}}, \quad \lambda > 0, \qquad (2.4)$$

which is responsible for the logarithmic corrections in the correlators in the case of a single spin chain is usually discarded when there are more relevant terms (such as those arising in the normal ladders from the interchain coupling). In the present case, though, it should be kept since the zig-zag interchain coupling gives rise only to marginal perturbations.

More precisely, the zig-zag coupling

$$H_{\mathrm{int}} = J'\sum_x \mathbf{S}^1_x\cdot(\mathbf{S}^2_x + \mathbf{S}^2_{x+1}), \qquad (2.5)$$

leads to the (marginal) current-current interaction

$$H_{\mathrm{int}} = \alpha\int \mathrm{d}x(\mathbf{J}^1_{\mathrm{R}} + \mathbf{J}^1_{\mathrm{L}})\cdot(\mathbf{J}^2_{\mathrm{R}} + \mathbf{J}^2_{\mathrm{L}}), \qquad (2.6)$$

where α is small and proportional to the interchain coupling J'. It is positive for antiferromagnetic coupling and negative for a ferromagnetic coupling. Discarding non-Lorentz invariant terms, which do not contribute to the one-loop renormalization group (RG) equations, one can rewrite the Hamiltonian in the following way

$$H = H^1_0 + H^2_0 - \beta\sum_{i=1}^{2}\int \mathrm{d}x(\mathbf{J}^i_{\mathrm{R}}\cdot\mathbf{J}^i_{\mathrm{L}}) + \alpha\int \mathrm{d}x\mathbf{J}^T_{\mathrm{R}}\cdot\mathbf{J}^T_{\mathrm{L}} \qquad (2.7)$$

where $\beta = \lambda + \alpha$ and $\mathbf{J}^T = \mathbf{J}^1 + \mathbf{J}^2$ which satisfies a level 2 Kac-Moody algebra. Equation (2.7) is the Hamiltonian considered in [22,23]. By a one-loop RG analysis one finds an exponentially small gap for antiferromagnetic zig-zag coupling and a massless regime for a ferromagnetic coupling. However, in [24] it was shown that there is another (marginal) term

$$\gamma\int \mathrm{d}x\left(\mathrm{tr}(\boldsymbol{\sigma}g^1)\cdot\partial_x\mathrm{tr}(\boldsymbol{\sigma}g^2) - \mathrm{tr}(\boldsymbol{\sigma}g^2)\cdot\partial_x\mathrm{tr}(\boldsymbol{\sigma}g^1)\right), \qquad (2.8)$$

with $\gamma \propto J'$, that could change the behaviour of the system in the ferromagnetic regime.

Now we proceed to discuss how the RG equations of [23] are changed when the chirally asymmetric perturbation term (2.8) is included in the non-Abelian bosonization framework. Such a computation was actually already performed in [24] using a fermionic representation. Still, our result will be complementary to [24] and is specially appropriate to analyze the $SU(2)$ symmetric case and generalize it to $N > 2$ since this symmetry is explicit in the present analysis.

It is easy to see that another $SU(2)$ invariant operator given by

$$\gamma'\int \mathrm{d}x\left(\mathrm{tr}(g^1)\partial_x\mathrm{tr}(g^2) - \mathrm{tr}(g^2)\partial_x\mathrm{tr}(g^1)\right), \qquad (2.9)$$

has to be included as a counterterm in the action. Using the operator product expansion of these operators and a rescaling of the coupling constants, one obtains the RG equations:

$$\frac{\mathrm{d}\alpha}{\mathrm{d}\ln\ell} = \alpha^2 + \gamma^2,$$
$$\frac{\mathrm{d}\beta}{\mathrm{d}\ln\ell} = -\beta^2 + 2\alpha\beta + \gamma^2,$$
$$\frac{\mathrm{d}\gamma}{\mathrm{d}\ln\ell} = 2\gamma\alpha + 2\gamma\beta + 2\gamma'\alpha,$$
$$\frac{\mathrm{d}\gamma'}{\mathrm{d}\ln\ell} = 6\gamma\alpha - 6\gamma'\beta + 6\gamma'\alpha. \qquad (2.10)$$

The RG equations obtained in [23] can be recovered from here by just putting $\gamma = \gamma' = 0$. It can be shown that for an AF coupling the presence of these γ and γ' terms does not affect the qualitative behaviour of the flow. The system is driven to a strong coupling regime, corresponding to the massive behaviour mentioned in [23]. The way terms like (2.8) affect the nature of the massive excitations in this strong coupling regime is nevertheless not so clear.

These equations can be generalized to an arbitrary number of coupled chains, provided all the chains are coupled in the same way. This applies in particular to $N = 3$ with periodic boundary conditions (PBC). One can then conclude that three chains with a periodic arrangement of antiferromagnetic coupling $J' > 0$ are massive at least in the weak-coupling region $J' \ll J$. Due to the dimensions of the perturbing operators involved, this kind of coupling can be considered as weaker than the normal coupling, in the sense that the growth of the associated coupling is governed by a smaller exponent in the present case. This shows the importance of a careful treatment of the marginal interactions. This should help to clarify the problem of the presence of a gap in the weak-coupling region for the usual $N = 3$ ladder with PBC.

The situation for a ferromagnetic coupling is more subtle. One can see that the trivial massless infrared fixed point $\alpha = \beta = 0$ is stable only if $\gamma = \gamma' = 0$. Then the presence of the twist term affects the large scale behaviour of the system, preventing it to reach the trivial massless point. So, the one-loop RG flows for weak $J' < 0$ and $J' > 0$ become similar. This has already been noticed in [24] where it was argued that the dimerized phase seems to extend into the ferromagnetic region. One should however keep in mind that this is just a one-loop calculation and non-perturbative effects could change the large scale behaviour of the system.

We conclude the present section stressing that all these results are easily generalizable to the weak-coupling regime of an arbitrary number N of coupled chains, provided that in the continuum limit all chains are coupled in an equal manner. It should be noted, however, that on the lattice, inequivalent versions of completely symmetric zig-zag interchain coupling exist for $N > 2$. After taking the continuum limit, these differences manifest themselves in different signs for interaction terms of the type (2.8), *i.e.* most of the originally completely symmetric boundary conditions are not symmetric anymore after taking the continuum limit. Note also that the cases of PBC where not all pair-couplings are present (which is the case for $N > 3$) or open boundary conditions (OBC) for $N > 2$ are much more subtle and it is not clear if the above results apply also to them.

2.2 The XXZ case

Let us consider now the addition of an XXZ anisotropy. In this case, the $SU(2)$ symmetry of the system is broken and it is then more appropriate to adopt the Abelian bosonization approach. Below we follow the notations of [36,22] in order to simplify making the connection with the non-Abelian description in terms of WZW fields of the previous section (this implies some minor changes of conventions such as a rescaling of the fields with respect to our study of the ordinary spin ladders [13]).

In the Abelian bosonization language, each chain is described by a compactified free bosonic field ϕ^i with its dynamics governed by[1]

$$H = \frac{1}{2}\int \mathrm{d}x \left(vK(\partial_x \tilde{\phi})^2 + \frac{v}{K}(\partial_x \phi)^2 \right). \tag{2.11}$$

The field ϕ^i and its dual $\tilde{\phi}^i$ are given by the sum and difference of the lightcone components, respectively. The constant K governs the conformal dimensions of the bosonic vertex operators and can be obtained exactly from the Bethe ansatz solution of the XXZ chain (see *e.g.* [13] for a detailed summary). We have $K = 1$ for the $SU(2)$ symmetric case ($\Delta = 1$) and it is related to the radius R of [13] by $K^{-1} = 2\pi R^2$.

In terms of these fields, the spin operators read

$$S^z_{i,x} = \frac{1}{\sqrt{2\pi}}\partial_x \phi^i + a : \cos(2k^i_{\mathrm{F}} x + \sqrt{2\pi}\phi^i) : + \frac{\langle M^i \rangle}{2}, \tag{2.12}$$

$$S^{\pm}_{i,x} = (-1)^x : \mathrm{e}^{\pm \mathrm{i}\sqrt{2\pi}\tilde{\phi}^i} \left(b \cos(2k^i_{\mathrm{F}} x + \sqrt{2\pi}\phi^i) + c \right) :, \tag{2.13}$$

where the colons denote normal ordering with respect to the groundstate with magnetization $\langle M^i \rangle$. The Fermi momentum k^i_{F} is related to the magnetization of the ith chain as $k^i_{\mathrm{F}} = (1 - \langle M^i \rangle)\pi/2$. The effect of an XXZ anisotropy and/or the external magnetic field (to be discussed later) is then to modify the scaling dimensions of the physical fields through K and the commensurability properties of the spin operators, as can be seen from (2.12), (2.13). The non-universal constants a, b and c can be in general computed numerically (see *e.g.* [37], for the case of zero magnetic field) and in particular the constant b has been obtained exactly in [38].

At zero magnetization, (*i.e.* $k^i_{\mathrm{F}} = \pi/2$), the first and second terms in each of these equations correspond to the components of the non-oscillatory ($\mathbf{J}^i_{\mathrm{R}} + \mathbf{J}^i_{\mathrm{L}}$) and oscillatory ($\mathrm{tr}(\boldsymbol{\sigma} g^i)$) terms in (2.3).

Let us consider now a two-leg zig-zag XXZ ladder. The perturbation terms in the case of zero magnetization can be separated into three classes:

(i) Terms quadratic in the derivatives

$$\alpha \partial_x \phi^1(x) \partial_x \phi^2(x), \tag{2.14}$$

that can be absorbed into a renormalization of the compactification radii, once we diagonalize the derivative part going to the new variables $\phi^{\pm} = (\phi^1 \pm \phi^2)/\sqrt{2}$. The K parameters are then renormalized as

$$K_{\pm} = K\Big(1 \mp 2J'K/(J\pi) + O\big((J'/J)^2\big)\Big). \tag{2.15}$$

(ii) The other contributions from current-current intrachain and interchain interactions can be rewritten as

$$\begin{aligned} &- \lambda \cos(\sqrt{4\pi}\phi^+) \cos(\sqrt{4\pi}\phi^-) \\ &+ \alpha \cos(\sqrt{4\pi}\tilde{\phi}^-) \left(\cos(\sqrt{4\pi}\phi^+) + \cos(\sqrt{4\pi}\phi^-) \right). \end{aligned} \tag{2.16}$$

[1] Note that a factor $(4R)^{-2}$ is missing in front of the Π^2 term in equations (2.2) and (3.4) of [13].

The dimensions of these operators are given by

$$K_+ + K_- \quad \text{and} \quad \frac{1}{K_-} + K_+, \tag{2.17}$$

respectively (the third operator in (2.16) is always irrelevant). The λ term (which is the standard current-current term for the individual chains) is irrelevant for $\Delta < 1$, while the α term is irrelevant for a ferromagnetic interchain coupling, except for $K = 1$ (and $J' = 0$) which corresponds to the $SU(2)$ symmetric point where it is marginal. For an AF coupling, the α term is relevant for $\Delta \geq 1$.

(iii) We also have chirally asymmetric terms [24] (those corresponding to (2.8)) which now read

$$-\partial_x\phi^+(x)\sin(\sqrt{4\pi}\phi^-); \quad +\partial_x\phi^-(x)\sin(\sqrt{4\pi}\phi^+); \quad -\partial_x\tilde{\phi}^+(x)\sin(\sqrt{4\pi}\tilde{\phi}^-). \tag{2.18}$$

Their dimensions are

$$1 + K_-, \quad 1 + K_+, \quad \text{and} \quad 1 + \frac{1}{K_-}\cdot \tag{2.19}$$

If we consider a small XXZ anisotropy with $\Delta \ll 1$, both $K_\pm$ increase and the term

$$\partial_x\tilde{\phi}^+(x)\sin(\sqrt{4\pi}\tilde{\phi}^-)$$

will now become the most relevant for sufficiently small J'.

Following arguments similar to the ones of [24] it follows that at most the symmetric (ϕ^+) sector is massless. For $\Delta > 1$, also this field acquires a mass, but stays massless for $\Delta \ll 1$. The above analysis cannot directly be applied to the region $\Delta \approx 1$, because higher loops should be included. Moreover, at the point $\Delta = 1$, the $SU(2)$ symmetry is not directly explicit in this treatment. However, according to the one-loop RG analysis in [24] and Section 2.1 of the present paper, a gap seems to open at $\Delta = 1$ for small $|J'| \neq 0$, regardless of its sign.

3 Stability of the zig-zag coupling and magnetization plateaux

In the present section we will study different mechanisms due to which the zig-zag interchain coupling becomes unstable against the perpendicular interchain coupling.

The outcome is that only under very special circumstances the zig-zag coupling is stable, while under the action of an external magnetic field, the addition of rung dimerization or the presence of charge carriers, an effective perpendicular coupling is generated.

3.1 XXZ in a magnetic field

When we add an external magnetic field to the XXZ zig-zag ladder, the situation is more subtle, since the staggered terms do not necessarily cancel. Indeed, we show in this section that new non-oscillating commensurate terms arise.

The current-current terms become

$$\sin k_{\mathrm{F}}\cos(\sqrt{4\pi}\tilde{\phi}^-)\Big(\sin k_{\mathrm{F}}\cos(\sqrt{4\pi}\phi^+ + 4k_{\mathrm{F}}x) + \sin(k_{\mathrm{F}} - \sqrt{4\pi}\phi^-)\Big), \tag{3.1}$$

and the other terms become

$$\begin{aligned}&-\partial_x\phi^+(x)\sin(2k_{\mathrm{F}} - \sqrt{4\pi}\phi^-)\\ &-\frac{1}{\sqrt{2}}\Big(\partial_x\phi^2(x)\sin(4k_{\mathrm{F}}x + 2k_{\mathrm{F}} + \sqrt{4\pi}\phi^+) - \partial_x\phi^1(x)\\ &\times\sin(4k_{\mathrm{F}}x - 2k_{\mathrm{F}} + \sqrt{4\pi}\phi^+)\Big) - \partial_x\tilde{\phi}^+(x)\sin(\sqrt{4\pi}\tilde{\phi}^-).\end{aligned} \tag{3.2}$$

The main difference with the case at $\langle M\rangle = 0$ is that now we have a very relevant term which is proportional to

$$\cos^2 k_{\mathrm{F}}\cos(4k_{\mathrm{F}}x + \sqrt{4\pi}\phi^+) + \cos k_{\mathrm{F}}\cos(k_{\mathrm{F}} - \sqrt{4\pi}\phi^-) \tag{3.3}$$

with dimensions K_+ and K_-. Note that the first term in (3.3) will disappear since it is incommensurate for $\langle M\rangle \neq 0$. Hence this term gives a mass to the ϕ^- field, leaving only the symmetric field massless.

We can then make the following statement about the phase diagram of two zig-zag coupled XXZ spin chains with $\Delta < 1$: For non-zero magnetization, and in all cases, one of the degrees of freedom is massive and the other massless, leaving a $c = 1$ theory.

With some modifications to the argumentation of [13], this can be easily generalized to N weakly coupled zig-zag chains, provided all the chains are coupled together: The generalization of the most relevant interaction term (3.3) to the case of N-leg ladders is:

$$\sum_{i,j}\Big\{\lambda_1\cos^2 k_{\mathrm{F}} : \cos\big(4xk_{\mathrm{F}} + \sqrt{2\pi}(\phi_i + \phi_j)\big) : + \lambda_2\cos k_{\mathrm{F}} : \cos\big(k_{\mathrm{F}} - \sqrt{2\pi}(\phi_i - \phi_j)\big) :\Big\}. \tag{3.4}$$

As for the case $N = 2$, the coupling constants λ_i essentially correspond to the coupling J' between the chains: $\lambda_i \sim J'/J$, but have a non-trivial dependence on $\langle M\rangle$: $\lambda_i \to 0$ for $\langle M\rangle \to 0$. The Gaussian part of the Hamiltonian is now given by:

$$\bar{H}^{(N)} = \int \mathrm{d}x\left[\frac{v}{2}\sum_{i=1}^{N}\left\{K\left(\partial_x\tilde{\phi}^i(x)\right)^2 + \frac{1}{K}\big(\partial_x\phi^i(x)\big)^2\right\} + \frac{\lambda}{\pi}\sum_{i,j}\big(\partial_x\phi_i(x)\big)\big(\partial_x\phi_j(x)\big)\right], \tag{3.5}$$

where $\lambda \sim J'/J$. As for the case of the normal coupled ladder, the last term produces a shift of the compactification radii of the fields and plays a crucial rôle in the opening of

non-trivial plateaux. In arriving to the Hamiltonian (3.5) we have discarded a constant term and absorbed a term linear in the derivatives of the free bosons into a redefinition of the applied magnetic field. One has also to include the generalization to N chains of the current-current term and the twist term. While obtaining the expression for the first one is an easy task, writing down the twist term for generic N has some subtleties. Keeping only commensurate terms, a naïve generalization of (2.18) would be:

$$\sum_{i>j} -\partial_x(\phi_i+\phi_j)\sin\big(2k_{\rm F}-\sqrt{2\pi}(\phi_i-\phi_j)\big) - \partial_x(\tilde\phi_i+\tilde\phi_j)\sin\big(\sqrt{2\pi}(\tilde\phi_i-\tilde\phi_j)\big). \quad (3.6)$$

If we take into account only the most relevant perturbation term (3.4), the analysis is similar to the one of the normal ladder given in [13]. In particular, one can radiatively generate "N-Umklapp" terms like $\cos\Big(2x\sum_{i=1}^N k_{\rm F}^i+\sqrt{4\pi N}\psi_{\rm D}\Big)$, where $\psi_{\rm D}=\frac{1}{\sqrt{N}}\sum_{i=1}^N\phi_i$, which can give rise to the appearance of a plateau if (1.1) is satisfied with $V=N$, $S=1/2$.

The zero-loop analysis for the opening of such plateaux is basically the same as in [13]. Just the coefficient of the interaction arising from the smooth part acquires an extra factor of two. *Via* the Gaussian part of the Hamiltonian this replaces J' by $2J'$ in the dimension formula for the N-Umklapp term. In this way, we obtain for example, at $\Delta=1$, $J'_{\rm c}\approx 0.045J$ for the $\langle M\rangle=1/3$ plateau at $N=3$ and $J'_{\rm c}\approx 0.35J$ for $\langle M\rangle=1/2$ at $N=4$ and also for $\langle M\rangle=1/5$ at $N=5$. At this level one could expect the magnetization curves of zig-zag ladders to be very similar to the ones of normal ladders. There are however some subtleties which are not captured by this analysis. There are inequivalent ways of coupling a number $N\geq 3$ chains in a periodic zig-zag way. These inequivalent ways of PBC couplings correspond in the weak coupling field theoretical model to changing the relative signs, or what is equivalent, permuting chain indices in the expression of the twist term (3.6). Since the zero-loop treatment presented above does not take into account the twist term, it is obvious that we have to consider loop corrections to take into account this effect. A detailed RG treatment of this model taking into account the current-current and twist term is a difficult task beyond the scope of this paper. However, exact diagonalization of finite chains for a strong enough J'/J ratio will show that these inequivalent couplings can give rise to different behaviour in the presence of a magnetic field. Another problem is the extension of these results to OBC where we encounter the same limitations as for the normal ladders. We refer the reader to [13] for a detailed discussion of this point. We just mention here that the results above cannot be directly extrapolated to configurations with OBC. In this case one should therefore complement the present field theoretical analysis by other methods such as exact diagonalization.

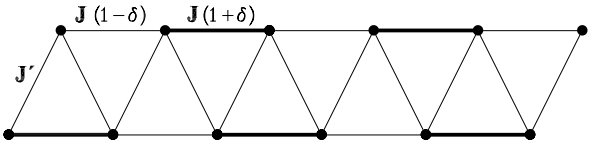

Fig. 2. Dimerization along the legs.

3.2 Dimerization in XXZ ladders

Another way to generate an effective perpendicular coupling is to include dimerization in the zig-zag coupling. Let us consider the Hamiltonian in (1.2) with non-zero rung dimerization δ. In the bosonized language, this gives rise to the perturbation term

$$H_{\rm dim}=J'\sum_i\sum_x\Big((-1)^x\mathbf{n}_i\cdot\big((1+\delta)(-1)^x\mathbf{n}_{i+1} + (1-\delta)(-1)^{x+1}\mathbf{n}_{i+1}\big)\Big)=2J'\delta\sum_i\sum_x\mathbf{n}_i\cdot\mathbf{n}_{i+1}, \quad (3.7)$$

where $\mathbf{n}_i$ is the staggered component of the spin operator at zero magnetization ($n_i^z=\cos(\sqrt{2\pi}\phi^i)$, $n_i^\pm=\exp(\pm{\rm i}\sqrt{2\pi}\tilde\phi^i)$).

This perturbation term can be rewritten as

$$H_{\rm dim}=\lambda\sum_i\sum_x\Big[-\cos\Big(\sqrt{4\pi}(\phi_i+\phi_{i+1})\Big) +\cos\Big(\sqrt{4\pi}(\phi_i-\phi_{i+1})\Big) +2\cos\Big(\sqrt{4\pi}(\tilde\phi_i-\tilde\phi_{i+1})\Big)\Big], \quad (3.8)$$

where $\lambda\propto J'\delta$.

The effective model is then very similar to the one for a ladder with a normal perpendicular coupling. In particular, using the formulae of [13], one can study the opening of plateaux in the magnetization curve as a function of δ and J'. The $N=2$ version of the dimerized zig-zag ladder has been analyzed in detail in [12] and the magnetization plateau with $\langle M\rangle=1/2$ predicted there was also observed numerically [39,40].

Another way to add dimerization is along the legs of the chains as in Figure 2, which gives rise to additional terms. They read in the presence of a magnetic field

$$\delta\sum_{i=1}^N\sum_x(-1)^x\cos\big(2k_{\rm F}x+\sqrt{2\pi}\phi^i\big), \quad (3.9)$$

which is incommensurate at non-zero magnetization, but can contribute to radiatively generated commensurate terms as we discuss below (see also [20]).

Taking as an example $N=2$, one can show that the operator

$$\lambda'\sum_x(-1)^x\cos\big(4k_{\rm F}x+\sqrt{4\pi}\phi^+\big) \quad (3.10)$$

is radiatively generated for non-zero magnetization, and it is commensurate for $\langle M\rangle = 1/2$. This operator arises from a combined effect of the interchain coupling and the dimerization along the chains and hence λ' in (3.10) is proportional to J', δ and $\langle M\rangle$. This operator has dimension K and is hence relevant, implying the existence of a plateau at 1/2 of the saturation magnetization.

A related analysis was performed in [9] but in the regime where the interchain coupling $J' \to -\infty$, which cannot be studied within the perturbative approach used here. In fact, in that case the existence of the plateau was associated with a different operator of higher dimension, which could become relevant only under certain conditions.

In the present case, the existence of the plateau is independent of the values of the microscopic parameters, since the dimension of the operator (3.10) is always smaller than 2. Furthermore, for a two-leg zig-zag ladder there is only one way to introduce dimerization along the legs and therefore in contrast to the ordinary ladders [20] cancellations do not occur.

An amusing observation which may also be of some relevance for experiments is that one recovers the two-leg zig-zag ladder with dimerized interchain coupling as the first-order effective Hamiltonian for the two-leg ladder with dimerization along the chains (see Fig. 2) in the limit of $\delta \to 1$. Details are given in an appendix. The main point is that dimerized interchain coupling and dimerization along the legs break translational symmetry in different ways: For the former case a translationally invariant unit cell of the Hamiltonian contains two spins while in the latter case it contains four. In view of the quantization condition (1.1), this suggests that dimerization along the legs can give rise to more plateaux than if only the interchain coupling is dimerized.

A similar analysis as the one of this section can be performed for generic N.

3.3 Doping with charge carriers

Let us consider now a generalization of the system studied in Section 2 by adding charge degrees of freedom. We start by describing the Hamiltonian of interacting electrons in one dimension [36,41]:

$$H = -\frac{D}{2}\sum_{x,\alpha}(c^\dagger_{x+1,\alpha}c_{x,\alpha} + \text{H.c.}) + U\sum_x c^\dagger_{x,+}c_{x,+}c^\dagger_{x,-}c_{x,-} \tag{3.11}$$

where $c^\dagger$ and c are electron creation and annihilation operators and $\alpha = \pm$. For positive U and at half filling, the charge sector is massive and the spin sector for large U can be described by the Heisenberg Hamiltonian [36]. Here, we will analyze the large scale behaviour of two identical systems coupled in zig-zag, away from half filling. Since we are now keeping the $SU(2)$ symmetry of the spin sector (neither magnetic field nor XXZ anisotropy will be considered), the continuum limit of the Hamiltonian at non-zero doping can be written as:

$$H = \frac{1}{2}\int \mathrm{d}x \left(v_\mathrm{c}K_\mathrm{c}(\partial_x\tilde{\phi}_\mathrm{c})^2 + \frac{v_\mathrm{c}}{K_\mathrm{c}}(\partial_x\phi_\mathrm{c})^2\right) + H_\mathrm{WZW}(g_\mathrm{s}) - \lambda\int \mathrm{d}x \mathbf{J}_\mathrm{R}\cdot\mathbf{J}_\mathrm{L}, \tag{3.12}$$

where the first term of the Hamiltonian stands for the charge sector and the WZW term describes the spin sector. The charge and spin density operators are given respectively by:

$$\rho(x) = j_\mathrm{R} + j_\mathrm{L} + \text{const. } \sin(2k_\mathrm{F}x + \sqrt{2\pi}\phi_\mathrm{c})\ \mathrm{tr}(g) + \text{const. } \cos(4k_\mathrm{F}x + \sqrt{8\pi}\phi_\mathrm{c}) \tag{3.13}$$

and

$$\mathbf{S}(x) = \mathbf{J}_\mathrm{R} + \mathbf{J}_\mathrm{L} + \text{const. } \sin(2k_\mathrm{F}x + \sqrt{2\pi}\phi_\mathrm{c})\ \mathrm{tr}(\boldsymbol{\sigma} g), \tag{3.14}$$

where j and $\mathbf{J}$ are the U(1) and $SU(2)$ currents of the charge and spin sector respectively. The Fermi momentum k_F is now related to the charge sector and we keep our spin sector at zero magnetization. It is known that $K_\mathrm{c} = 1$ for $U = 0$ and $K_\mathrm{c} = 1/2$ for $U = \infty$ [42].

We again consider two copies of the system and study perturbatively the zig-zag coupling between them. More precisely, we consider a coupling term which involves both charge and spin densities

$$H_\mathrm{int} = \sum_x \left(\frac{U'}{2}\rho^1_x(\rho^2_x + \rho^2_{x+1}) + J'\mathbf{S}^1_x(\mathbf{S}^2_x + \mathbf{S}^2_{x+1})\right).$$

The presence of a further direct hopping term between the chains would require a more detailed analysis. Indeed, first the Gaussian part must be diagonalized including this direct hopping term and then, for example, one can treat perturbatively terms like H_int. This is beyond the scope of the present article where we just concentrate on showing that the presence of a weak coupling between Hubbard chains like in [41] generalized to the zig-zag configuration can give rise to results similar to those observed for normal ladders.

In the continuum description, this interaction term can be written in two different pieces. We first have the current-current interaction term given by

$$\frac{U'}{2}(j^1_\mathrm{R} + j^1_\mathrm{L})(j^2_\mathrm{R} + j^2_\mathrm{L}) + J'(\mathbf{J}^1_\mathrm{R} + \mathbf{J}^1_\mathrm{L})\cdot(\mathbf{J}^2_\mathrm{R} + \mathbf{J}^2_\mathrm{L}). \tag{3.15}$$

The U(1) current-current term can be completely absorbed in the Gaussian charge Hamiltonian by a rescaling of v_c and K_c

$$K^\pm_\mathrm{c} = \left(1 \pm \frac{U'}{2\pi v_\mathrm{c}}\right)^{-1/2} K_\mathrm{c} \tag{3.16}$$

where the indices $\pm$ stand for the symmetric and antisymmetric fields $(\phi^1_\mathrm{c} + \phi^2_\mathrm{c})/\sqrt{2}$ and $(\phi^1_\mathrm{c} - \phi^2_\mathrm{c})/\sqrt{2}$ respectively.

The $SU(2)$ current term is identical to the one of Section 2.1 and we know then that it plays a rôle only for positive J'.

There is however another commensurate perturbation present away from half filling which is given by

$$\cos k_{\rm F}\ \cos(\sqrt{4\pi}\phi_{\rm c}^-)\big(U'\ \text{const.}\ \mathrm{tr}(g^1)\ \mathrm{tr}(g^2) + J'\ \text{const.}\ \mathrm{tr}(\boldsymbol{\sigma} g^1)\cdot\mathrm{tr}(\boldsymbol{\sigma} g^2)\big). \quad (3.17)$$

In the present case, the chirally asymmetric terms are irrelevant in the RG sense.

In the weak interchain coupling limit we are considering, U' is much smaller than U. Then $U'/(2\pi v_{\rm c}^-) < 1-K_{\rm c}^2$ and this term is relevant giving a mass to all the spin degrees of freedom as well as to the antisymmetric charge field $\phi_{\rm c}^-$. Thus, only the field $\phi_{\rm c}^+$ remains massless.

We see from (3.17) that also in this case an effective perpendicular coupling is generated, signaling the instability of the zig-zag interchain coupling also against charge doping.

Since the perturbation terms in (3.17) are the same as those that appear in the normal coupling studied in [41], it is then natural to expect that the IR behaviour of the charge density wave and superconducting correlation functions will be the same in the present case.

4 Numerical analysis of the two-leg case

In this section we consider the $N = 2$ version of (1.2) without dimerization, *i.e.* $\delta = 0$. It is then useful to think of the two-leg zig-zag ladder as a single chain with next-nearest neighbour interaction. So, for $N = 2$ the Hamiltonian (1.2) can be recast in the form (writing explicitly an XXZ anisotropy Δ)

$$H = J'\sum_{x=1}^{L}\left\{\Delta S_x^z S_{x+1}^z + \frac{1}{2}\left(S_x^+ S_{x+1}^- + S_x^- S_{x+1}^+\right)\right\} + J\sum_{x=1}^{L}\left\{\Delta S_x^z S_{x+2}^z + \frac{1}{2}\left(S_x^+ S_{x+2}^- + S_x^- S_{x+2}^+\right)\right\} - h\sum_{x=1}^{L} S_x^z. \quad (4.1)$$

Here L denotes the total volume of the system. In this section we will always assume $J > 0$. To avoid frustration also in the limit $J' \to 0$ where we find two weakly coupled chains, we choose L to be a multiple of 4.

In the formulation (4.1) essentially all spatial symmetries are manifestly implemented by a one-site translation $x \to x+1$. So, one can use Fourier transforms to simplify the determination of the spectrum. Since the magnetic field h is coupled to a conserved order parameter in (4.1), we can relate all quantities at a field h to those at $h = 0$ – the results to be reported below are all obtained from computations with $h = 0$.

There is already a number of exact diagonalization studies for the two-leg XXZ zig-zag ladder (or equivalently the Heisenberg chain with next-nearest-neighbour interactions) in a magnetic field [43–49,39]. However, there are still some regions in the parameter space and aspects which have not been studied in great detail, such that further numerical investigations seem worthwhile. For a numerical analysis we concentrate on the isotropic point $\Delta = 1$. It turns out that groundstate momenta can be incommensurate in the presence of the magnetic field. Such a feature is interesting in its own right and reminds us of recent observations made for the $S = 1$ chain with biquadratic interaction [50,51], but also gives rise to technical complications. This incommensurability is one reason why the computations to be reported below needed substantially more CPU time than analogous computations for conventional ladders [10], even though we used an improved version of the program employed loc.cit.

In order to scan the whole range of coupling constants we choose a normalization such that $J + |J'| = 1$. $J' = 0$ then corresponds to two decoupled chains, $J' = 1$ to a single antiferromagnetic chain and $J' = -1$ to a single ferromagnetic chain. The resulting magnetic phase diagram is shown in Figure 3. Here, the lines show the magnetic fields where the magnetization jumps between two different values that are realized at a given system size. The conclusions are schematically summarized in the inset of Figure 3. Regions with a ferromagnetically polarized groundstate are denoted by an "F". The other regions will be explained in the following discussion of our results.

Let us look first at the antiferromagnetic region $J' > 0$. Here spins flip one after the other. The groundstate momenta are in general incommensurate (*i.e.* not multiples of $\pi/2$) in the region IC1 ($0 < J' < 4J$), though for the small lattice sizes accessible to us, this does not show up in the region of small J'. For $h = 0$, a study of the static structure factor exhibited a transition to incommensurate behaviour at $J'/J \approx 1.92075$ [52].

For $h > 0$, the onset of incommensurability in the groundstate momenta was determined in [47], and [53] determined a transition in the groundstate using a different criterion. In the incommensurate region IC1 of Figure 3, the lines are irregular which is mainly due to the lattice discretization of the momenta. In the region C1, *i.e.* for $J' > 4J$, all groundstate momenta are commensurate and convergence with system size is good.

A gap [21,22] can be anticipated in Figure 3 for $J \le J' \le 2J$, but apart from that there is no evidence for any non-trivial plateaux. In fact, non-trivial plateaux have not been observed at the various points which have been studied over the past decade [39,43,44,46,49]. These observations can be nicely interpreted in terms of the quantization condition (1.1). In view of the mapping to a single chain (4.1), one should substitute $N = 1$ in (1.1). The gap then arises by spontaneous breaking of this enhanced translational symmetry to $l = 2$. Non-trivial plateaux would then require $l > 2$, which at least in the two-leg zig-zag ladder does not seem to be permitted.

The magnetization process on the ferromagnetic side has already been looked at some time ago [45], though no definite conclusion was reached due to problems of resolution. Indeed, the ferromagnetic side is quite a bit different from the antiferromagnetic one, even though

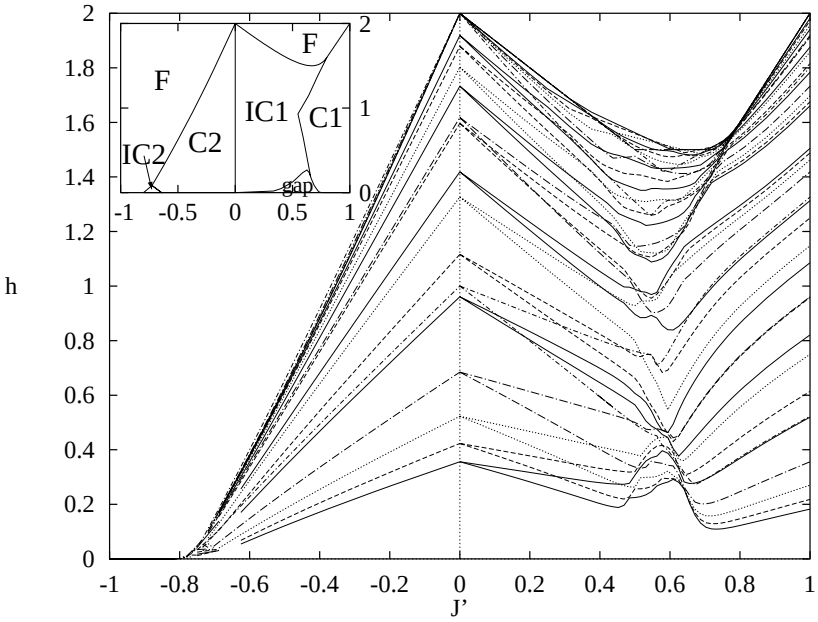

Fig. 3. Magnetic phase diagram with the choice of normalization $J + |J'| = 1$. The lines are for $L = 24$ (full), $L = 20$ (dashed). $L = 16$ (dotted), $L = 12$ (long dashed-dotted) and $L = 8$ (dashed-dotted). The inset shows a schematic version which is discussed in the text.

plateaux do neither seem to occur here. In the region C2 ($-3J/2 \leq J' < 0$), spins flip in pairs and the groundstate momenta of those states that participate in the magnetization process are commensurate (actually 0 or $\pm\pi$). The states with an odd number of spins pointing up (or down) can have incommensurate momenta, but they do not participate in the magnetization process.

At $J' = -4J$ a transition to a completely polarized ferromagnet takes place. The precise location of the transition point can be attributed to the fact that at $J' = -4J$ an exact $S = 0$ groundstate, the uniformly distributed RVB state [54] can be written down and is degenerate with the ferromagnetic state. The intermediate region IC2 (*i.e.* roughly $-4J < J' < -3J/2$) is rather complicated: Here the number of spins flipping simultaneously at a given system size changes with J'/J. Furthermore, groundstates with incommensurate momenta (*i.e.* momenta not an integer multiple of π) do participate in the finite-size magnetization process.

The magnetization process in the region IC2 is illustrated in Figure 4 by the finite-size magnetization curves at $J' = -3J$. Here, the number of spins that flip simultaneously in a finite-size system varies between 1 and 3 (the number of spins flipping simultaneously increases as one approaches $J' = -4J$). Strong non-monotonic finite-size effects can be observed in particular at the smaller system sizes. Nevertheless, a reasonable approximation to the limit $L \to \infty$ seems to be obtained applying the procedure of [55] to $L = 20$ and $L = 24$, *i.e.* by connecting the midpoints of the steps in the finite-size magnetization curves. This yields the bold line in Figure 4. The behaviour at small fields is somewhat speculative since the finite-size gaps are non-monotonic such that it is not possible to extrapolate them. We have therefore simply assumed a vanishing gap in the limit $L \to \infty$.

The region close to saturation in Figure 4 is on comparably safe grounds. In fact, we have data for up to $L = 48$ which has been taken into account for the bold curve. In the case $J' = -3J$, this data yields no evidence for more than three spins flipping simultaneously at the transition $\langle M \rangle \to 1$. Therefore we are confident that the magnetization curve becomes smooth in the thermodynamic limit (though very steep at the transition $\langle M \rangle \to 1$). In particular, we think that our intermediate phase IC2 is different from the metamagnetic one observed in [48] in a different parameter region, even though at first sight they bear some resemblance. The fact that we are not aware of any evidence for incommensurate momenta arising in the metamagnetic phase [48] also suggests that there are two distinct phases preceding a transition to a ferromagnet in different parameter regions.

We would like to conclude the present discussion with a few remarks on the spin-gap. Although it has already been investigated with high accuracy for $J' > 0$ applying the density matrix renormalization group to large system sizes [21,22,25], there are still some interesting problems. Firstly, only two of these investigations [21,22] deal with the incommensurate region and there the results differ by more than 10%. Secondly, no such investigations were performed for $J' < 0$. In these two regions, $S = 1$ excitations (corresponding to the lowest lines in Fig. 3 for $J' > 0$) have an incommensurate momentum at the minimum of their dispersion. Since the system size limits the resolution in momentum-space, one has additional non-monotonic finite-size effects. We have tried to overcome this with an interpolation using a Fourier transform of the dispersion. However, even/odd momentum effects (which are characteristic for scattering states) obscure the true incommensurate minimum and preclude such an analysis. According to preliminary investigations, such an approach

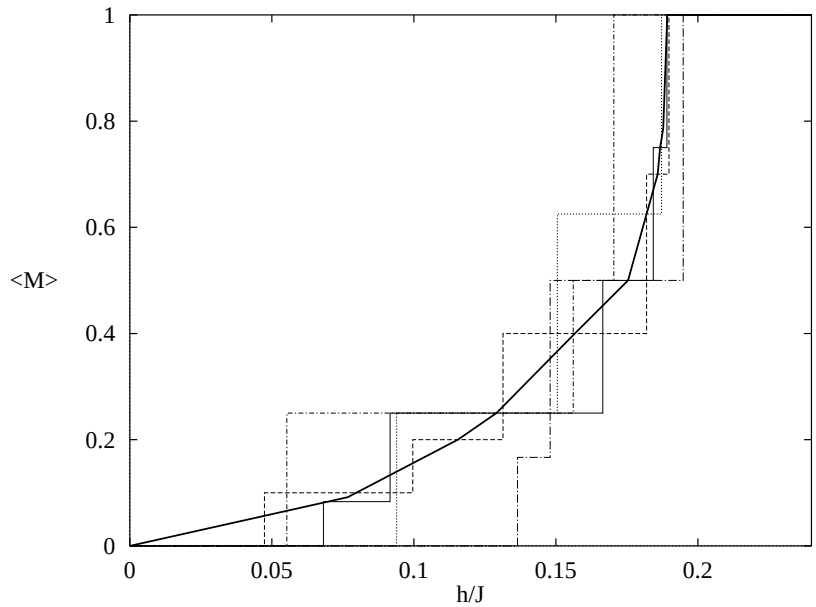

Fig. 4. Magnetization curves at $J' = -3J$ with lines for $L = 24$ (full), $L = 20$ (dashed). $L = 16$ (dotted), $L = 12$ (long dashed-dotted) and $L = 8$ (dashed-dotted). The bold line is a sketch of the form expected in the thermodynamic limit.

is applicable to $S = 1/2$ excitations (the fundamental spinon-type excitations) not only in the commensurate region [25] but also in the incommensurate region.

The question of a spin-gap is particularly interesting for $J' < 0$. In Section 2.1 we have confirmed the conclusion of [24] that a one-loop RG analysis suggests a non-zero spin-gap for small $J' < 0$. However, for $J' < 0$ there is no region where a gap in the magnetic excitations is obvious from our numerical data. The data for the $S^z = 2$ excitations (corresponding to the lowest lines for $J' < 0$ in Figure 3) actually fits well to the form

$$\mathsf{E}(L) \sim \frac{1}{L} \cdot \tag{4.2}$$

Such a form is characteristic for a conformally invariant and thus gapless situation (see *e.g.* [56]). For this reason we have not drawn a gap in the schematic inset of Figure 3 for $J' < 0$. Nevertheless, it remains a challenge to find numerical evidence for a spin-gap in some magnetic excitations and look for possible massless sectors which should be organized into $\widehat{su(2)}_1$ representations.

5 The transition to saturation in the two-leg ladder

5.1 The antiferromagnetic side

Now let us look at the transition to saturation in the lattice-version of the $N = 2$-leg zig-zag ladder.

First we recall the computation of the transition field $h_{\rm uc}$ [48]. One can immediately write down the energy of a fully polarized (ferromagnetic) state (with $h = 0$)

$$E_{\rm sat} = \frac{L}{4} \Delta \left(J' + J \right). \tag{5.1}$$

Using a Fourier transform, also the excitation energy of a single spin-wave above this fully polarized state is readily computed as

$$\mathcal{E}_{1s}(p) = -\Delta \left(J' + J \right) + J' \cos p + J \cos(2p). \tag{5.2}$$

To determine the critical magnetic field $h_{\rm uc}$ associated to the transition $\langle M \rangle \to 1$, we have to minimize (5.2). One finds the minimum at

$$p_{\rm min} = \begin{cases} \pi - \cos^{-1}\left(\dfrac{J'}{4J} \right) & \text{for } \ 0 \le J' \le 4J, \\ \pi & \text{for } \ J' \ge 4J. \end{cases} \tag{5.3}$$

An immediate consequence of this simple result is that the groundstate of the $S^z = L - 1$ sector has an incommensurate momentum for $0 < J' < 4J$. This is presumably the simplest example of how the two competing interactions in (4.1) lead to the phase with incommensurate groundstate momenta which we discussed in the previous section.

Insertion of (5.3) into (5.2) directly leads to the upper critical field

$$h_{\rm uc} = \begin{cases} \Delta J' + (\Delta + 1) J + \dfrac{{J'}^2}{8J} & \text{for } \ 0 \le J' \le 4J, \\ (\Delta + 1) J' + (\Delta - 1) J & \text{for } \ J' \ge 4J. \end{cases} \tag{5.4}$$

Now we will go beyond [48] and discuss the nature of the transition $\langle M \rangle \to 1$. To this end, it is useful to look at two-spinwave excitations [57]. After a Fourier transformation, one arrives at a matrix problem in the distance of the two flipped spins. We omit the explicit expressions for the matrices that we have used to study the behaviour of the magnetization curve close to saturation. This is equivalent to studying the finite-size behaviour of the two-spinwave groundstate energy $\mathcal{E}_{2s}$ at $h = h_{\rm uc}$, since $1 - \langle M \rangle = 4/L$ and $\mathcal{E}_{2s} = h - h_{\rm uc}$.

For the two-leg zig-zag ladder, the eigenvalue problem in the two-spinwave subspace can be interpreted as a fourth-order difference equation with suitable boundary conditions and thus can in principle be solved by a further Fourier transformation. For our purposes it turned out to be sufficient to fix the center-of-mass momentum p and then perform a numerical diagonalization for system sizes up to $L \approx 150$. We have looked at $\Delta = 1$ and the following values of the coupling constants: $J' = 2J$, $J' = 4J$, $J' = 4.1J$ and $J' = 4\cos(\pi/12)J$. These values were selected since for them (5.3) can be realized exactly for suitable choices of the system size L and one can thus avoid further non-monotonic finite-size effects which could arise from the lattice discretization in momentum space. In all cases that we have studied, the minimum energy of the two-spinwave excitation was found in the sector with center-of-mass momentum $p = 0$.

The numerical diagonalization determines the critical field associated to the transition from two flipped spins to one flipped spin. For $J' \neq 4J$, this critical field is compatible with the universal DN-PT behaviour [58,59]

$$h_{\rm uc} - h \sim (1 - \langle M \rangle)^2. \tag{5.5}$$

Just at $J' = 4J$ we find a different behaviour which is much better described by[2]

$$h_{\rm uc} - h \sim (1 - \langle M \rangle)^4. \tag{5.6}$$

To understand why just the point $J' = 4J$ leads to a different exponent, it is instructive to look at the behaviour of $\mathcal{E}_{1s}$ near the minimum $p_{\rm min}$. From (5.2) and (5.3) we find

$$\mathcal{E}_{1s}(p_{\rm min} + x) - \mathcal{E}_{1s}(p_{\rm min}) = \begin{cases} \dfrac{(4J - J')(4J + J')}{8J} x^2 + \mathcal{O}(x^3) & \text{for } J' < 4J, \\ \dfrac{J}{2} x^4 + \mathcal{O}(x^6) & \text{for } J' = 4J, \\ \left(\dfrac{J'}{2} - 2J \right) x^2 + \mathcal{O}(x^4) & \text{for } J' > 4J. \end{cases} \tag{5.7}$$

We see that the dispersion is quadratic everywhere except for the point $J' = 4J$ where it is quartic. These exponents in the one-spinwave dispersion are in one-to-one correspondence with those in (5.5) and (5.6), respectively. So, the behaviour of the magnetization for $\langle M \rangle \to 1$ can be explained by the band structure. Note that (5.7) is independent of Δ, and so should be the exponents corresponding to (5.5, 5.6), respectively (as long as $\Delta > 0$).

5.2 The ferromagnetic side

Now we turn to the transition to saturation on the ferromagnetic side $J' < 0$. Since we know from the numerical investigation that spins flip in pairs (as long as $|J'|$ is not too large), we have to solve a non-trivial matrix problem already to determine the critical field $h_{\rm uc}$ in the ferromagnetic regime $J' < 0$. For $|J'| < 2.5J$, the minimum of the dispersion of the two-spinon state is now located at $p = \pi$. In the region $J' < -2.66J$, the minimum moves away form $p = \pi$, *i.e.* it becomes incommensurate. In the following we restrict ourselves to the region of sufficiently small $|J'|$ such that spins flip in pairs and only commensurate groundstates participate in the magnetization process for $\langle M \rangle \to 1$.

Some values of transition fields $h_{\rm uc}$ are listed in Table 1. These have actually been obtained on chains with a few hundred sites. Nevertheless, all given digits should be those of the thermodynamic limit.

To check the asymptotic behaviour of the magnetization curve, one further needs at least the transition field $h_{4\to 2}$ at which two spins flip to reduce the number of spins deviating from the ferromagnetic state from four to two. Table 1 lists transition fields $h_{4\to 2}$ computed numerically on chains with $36 \leq L \leq 72$. Since $1 - \langle M \rangle \sim 1/L$, we can then test for the universal behaviour (5.5) by forming the expression

$$L\sqrt{h_{\rm uc} - h_{4\to 2}}, \tag{5.8}$$

which should converge to a constant if (5.5) is satisfied. Indeed, the expression (5.8) appears to converge to a constant with increasing L for all cases listed in Table 1. So, we find no counterevidence against the universal DN-PT behaviour on the ferromagnetic side either, although we have no compelling argument in its favour.

We expect that the transition $\langle M \rangle \to 1$ remains second order if we increase $|J'|$ further into the regime where more than two spins flip at the same time (this is in contrast to the metamagnetic transition studied in [48]). At least in this region the very steep behaviour of the magnetization curve (see Fig. 4) could mean a breakdown of the DN-PT universal behaviour (5.5). However, due to the flipping of several spins at the same time, we are not able to investigate the transition to saturation in detail numerically in this region.

6 The three-leg case

Now we proceed with a discussion of $N = 3$-leg zig-zag ladders on the lattice, though in less detail than for the two-leg ladder. For $N = 3$ there is a large number of possible boundary conditions for the coupling between the chains. In particular for periodic boundary conditions (PBC), there are several possibilities already for $N = 3$, of which none is naturally singled out in the case of zig-zag coupling. We will discuss three types of PBC in addition to open boundary conditions along the rungs. To elucidate these different types of boundary conditions it may be useful to consider the case $J' = J$ where the three-leg zig-zag ladder can be considered as a strip of the triangular lattice Heisenberg antiferromagnet. The triangular lattice has three sublattices and it is possible to consider boundary conditions that do or do not respect this sublattice structure. We will call the PBC that respect this

[2] The exponent 4 has also been observed in [46] at $J'/J = 4$.

Table 1. Values of $h_{4\to 2}$ at which a transition from four to two spins deviating from the ferromagnetic state takes place at a given size L. The last row contains auxiliary data, *i.e.* values of $h_{\rm uc}$ which were estimated using much larger systems.

J'/J	0	$-3/13$	$-1/3$	$-5/11$	$-3/5$	$-7/9$	-1	$-9/7$	$-5/3$	$-11/5$
L	$h_{4\to 2}/J$									
36	1.96595	1.77368	1.69888	1.60799	1.50460	1.38523	1.24387	1.07095	0.85064	0.55455
40	1.97272	1.78215	1.70116	1.60981	1.50630	1.38682	1.24527	1.07208	0.85145	0.55495
44	1.97766	1.78427	1.70263	1.61109	1.50753	1.38796	1.24624	1.07287	0.85201	0.55522
48	1.98137	1.78568	1.70366	1.61204	1.50844	1.38879	1.24695	1.07343	0.85241	0.55542
52	1.98423	1.78666	1.70441	1.61277	1.50914	1.38941	1.24748	1.07385	0.85271	0.55556
56	1.98648	1.78736	1.70499	1.61335	1.50968	1.38988	1.24788	1.07418	0.85294	0.55567
60	1.98828	1.78788	1.70546	1.61381	1.51010	1.39025	1.24819	1.07443	0.85312	0.55576
64	1.98974	1.78828	1.70583	1.61418	1.51044	1.39054	1.24844	1.07463	0.85326	0.55582
68	1.99094	1.78859	1.70615	1.61448	1.51071	1.39078	1.24864	1.07479	0.85338	0.55588
72	1.99195	1.78885	1.70641	1.61473	1.51093	1.39097	1.24880	1.07492	0.85347	0.55592
$h_{\rm uc}/J$	2	1.79086	1.70833	1.61648	1.51250	1.39236	1.25000	1.07589	0.85417	0.55625

sublattice structure at $J'=J$ 'PBC of type A', while those that identify different sublattices 'PBC of type B and C'.

The $N=3$-leg zig-zag ladder with PBC of type B and C can be rewritten as a single Heisenberg chain with interactions up to distances of three, respective four sites:

$$\begin{aligned} H = J' \sum_{n=1}^{3L} \Big\{ & \Delta S_n^z S_{n+1}^z + \frac{1}{2}\left(S_n^+ S_{n+1}^- + S_n^- S_{n+1}^+\right) \\ & + \Delta S_n^z S_{n+r}^z + \frac{1}{2}\left(S_n^+ S_{n+r}^- + S_n^- S_{n+r}^+\right)\Big\} \\ & + J \sum_{n=1}^{3L} \Big\{ \Delta S_n^z S_{n+3}^z + \frac{1}{2}\left(S_n^+ S_{n+3}^- + S_n^- S_{n+3}^+\right)\Big\} \\ & - h \sum_{n=1}^{3L} S_n^z. \end{aligned} \tag{6.1}$$

Here the second interaction term goes over a distance $r=2$ for PBC of type B, while PBC of type C are characterized by $r=4$.

Due to (6.1), the three-leg zig-zag ladder with PBC of type B can be considered as the natural counterpart of the $N=2$ zig-zag ladder where the Hamiltonian can be written in the form (4.1).

In contrast to the preceding discussion of the two-leg case we will from now on again denote the length of each chain by L, *i.e.* the total number of spins is then $3L$. Accordingly, we introduce a momentum p by a one-site translation along one of the three chains.

In the following we will study each of these four boundary conditions in turn.

6.1 The saturation field

First, we compute the field $h_{\rm uc}$ at which the transition to saturation takes place. This is not only useful to check the numerical computation to be reported in the next subsection, but like in the case $N=2$ also serves as a guide where groundstates with incommensurate momenta can participate in the magnetization process.

6.1.1 PBC of type A

A simple computation yields the excitation energy of one flipped spin above a ferromagnetic background as

$$\begin{aligned} \mathcal{E}_{1s,\pm}(p) = & -2\Delta J' - \frac{J'}{2}\left(1+\cos(p) \pm \sin(p)\sqrt{3}\right) \\ & - \Delta J + J\cos(p). \end{aligned} \tag{6.2}$$

The minimum of this dispersion is located at

$$\tan\left(p_{\min,\pm}\right) = \pm \frac{J'\sqrt{3}}{J'-2J}, \tag{6.3}$$

which is generically incommensurate. This then leads to the transition field

$$\begin{aligned} h_{\rm uc} &= -\mathcal{E}_{1s,\pm}(p_{\min,\pm}) \\ &= \Delta\left(2J'+J\right) + \frac{J'}{2} + \sqrt{J'^2 - J'J + J^2}. \end{aligned} \tag{6.4}$$

6.1.2 Open boundary conditions

The three-leg zig-zag ladder with open boundary conditions is shown in Figure 1. Here we consider only the case without dimerization ($\delta=0$).

The dispersion of the gap corresponding to a single flipped spin above the ferromagnetic background is given by

$$\begin{aligned} \mathcal{E}_{1s}(p) = & -\Delta J + J\cos\left(p\right) \\ & - J'\left(\frac{3}{2}\Delta + \frac{1}{2}\sqrt{\Delta^2 + 8\cos\left(\frac{p}{2}\right)^2}\right). \end{aligned} \tag{6.5}$$

For $\Delta J < J' < J\sqrt{\Delta^2+8}$, this dispersion has an incommensurate minimum at

$$\cos\left(\frac{p_{\min}}{2}\right) = \frac{1}{4}\,\frac{\sqrt{2J'^2 - 2\Delta^2 J^2}}{J}\,. \tag{6.6}$$

This then leads to an upper critical field

$$h_{\rm uc} = -\mathcal{E}_{1s}(p_{\min}) = \left(\frac{\Delta}{2}+1\right)^2 J + \frac{J'^2}{4J} + \frac{3J'\Delta}{2}\,. \tag{6.7}$$

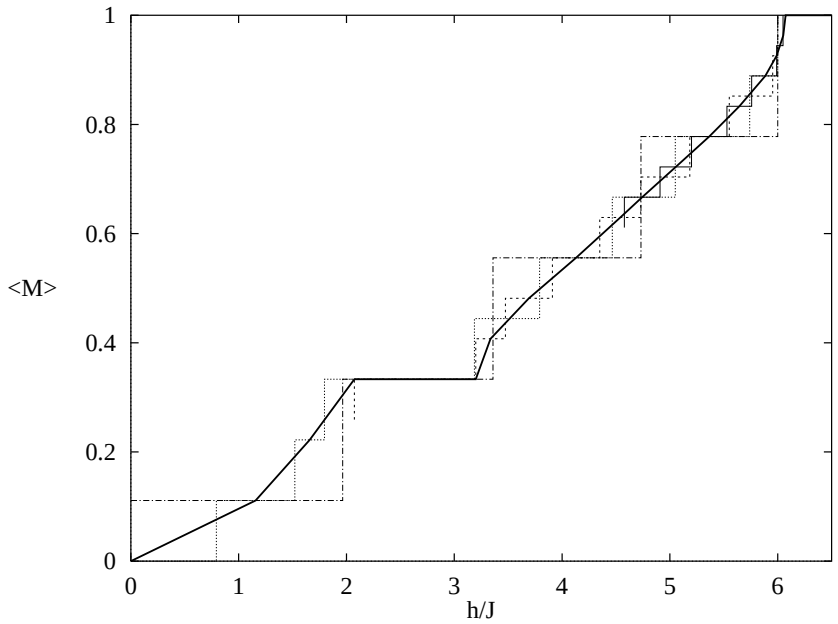

Fig. 5. Magnetization curves of an $N = 3$ zig-zag ladder with PBC of type A at $J' = 3J/2$. The lines are for $L = 12$ (full), $L = 9$ (dashed). $L = 6$ (dotted) and $L = 3$ (dashed-dotted). The bold line is an extrapolation to the thermodynamic limit.

6.1.3 PBC of type B and C

Using the representation (6.1) one easily finds the dispersion of a single flipped spin above the ferromagnetic background

$$\mathcal{E}_{1s}(p) = -\Delta(2J' + J) + J\cos(p) + J'\left\{\cos\left(\frac{rp}{3}\right) + \cos\left(\frac{p}{3}\right)\right\}. \quad (6.8)$$

Since the PBC of type B ($r = 2$) are simpler to discuss analytically, we will now concentrate on this case. The dispersion (6.8) then always has an incommensurate minimum at

$$\cos\left(\frac{p_{\min}}{3}\right) = \frac{\sqrt{J'^2 - 3JJ' + 9J^2} - J'}{6J}. \quad (6.9)$$

From this we find an upper critical field for PBC of type B

$$h_{\rm uc} = -\mathcal{E}_{1s}(p_{\min}) = \Delta(2J' + J) + \frac{J'\left(9JJ' - 2J'^2 + 27J^2\right)}{54J^2} + \frac{\left(J'^2 - 3JJ' + 9J^2\right)^{\frac{3}{2}}}{27J^2}. \quad (6.10)$$

6.2 Magnetization curves obtained by exact diagonalization

Now we present one example of a magnetization curve for each of the four boundary conditions introduced above. In all cases we consider the $SU(2)$ symmetric situation $\Delta = 1$ and set $J'/J = 3/2$.

6.2.1 PBC of type A

An example of a magnetization curve for $N = 3$ with PBC of type A is shown in Figure 5. For $J = J'$, this geometry is one of the possible approximations to a two-dimensional triangular lattice antiferromagnet and a study of precisely this geometry [60,61] exhibits a clear plateau with $\langle M\rangle = 1/3$. For $J = 0$, one recovers an 'ordinary' rectangular spin ladder with periodic boundary conditions which then has equal coupling constants. The latter has already been investigated in some detail [10,13,17] and evidence was found for a small plateau with $\langle M\rangle = 1/3$ (there is further the possibility of a tiny spin-gap at $h = 0$ [62,13]).

In Figure 5 we chose $J' = 3J/2$ in order to study a new example. One can see from (6.3) that this gives rise to an incommensurability for $\langle M\rangle \to 1$ (also at other values of the magnetization there is evidence that this choice of parameters lies in an incommensurate phase). Both at $J = 0$ and $J' = 0$, one should choose even L to avoid frustration by the periodic boundary conditions along the chains, while for $J' = J$ frustration is avoided if L is chosen to be a multiple of 3. To avoid both effects, L should be chosen as a multiple of 6. However, this would considerably restrict the system sizes accessible to us. We therefore require only divisibility by three (which seems to be the more important one if the coupling constants are of a similar magnitude).

The upper critical field for the choice of parameters in Figure 5 is evaluated from (6.4) as $h_{\rm uc}/J = 19/4 + \sqrt{7}/2 \approx 6.072\,9$.

Like for $N = 2$ in Figure 4, we applied the extrapolation procedure of [55] to the largest available system sizes in order to obtain the estimate for the magnetization curve in the thermodynamic limit which is shown by the bold line in Figure 3.

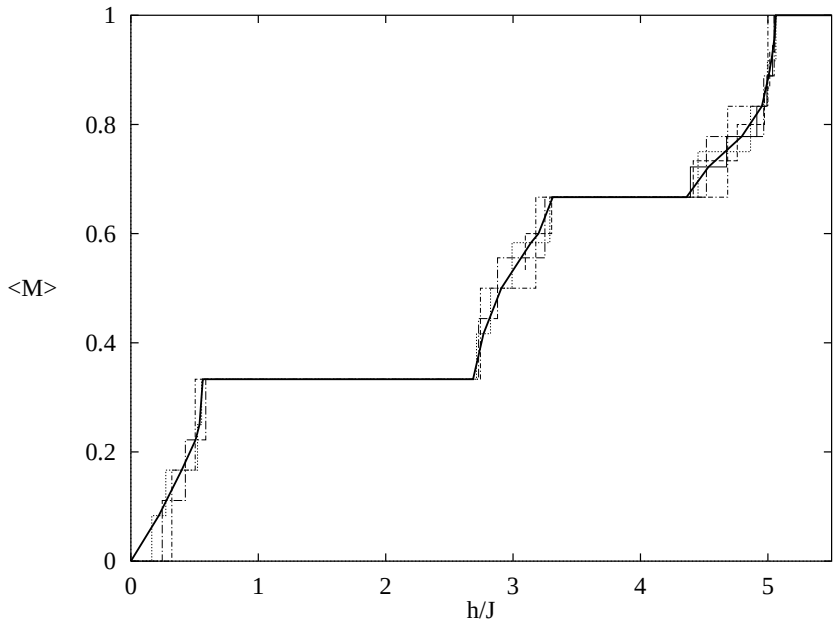

Fig. 6. Magnetization curves of an $N = 3$ zig-zag ladder with open boundary conditions along the rungs and $J' = 3J/2$. The lines are for $L = 12$ (full), $L = 10$ (dashed). $L = 8$ (dotted), $L = 6$ (long dashed-dotted) and $L = 4$ (dashed-dotted). The bold line is an extrapolation to the thermodynamic limit.

In this extrapolated magnetization curve we have only drawn an $\langle M\rangle = 1/3$ plateau but no further ones. This is motivated by the criterion (4.2): If we compare $\mathsf{E}(6) \approx 0.793J$ with $\mathsf{E}(4) \approx 1.274J$ (the latter is not shown in Fig. 3) we see that the decrease is faster than (4.2). These are only two data points which probably do not lie in the asymptotic regime (in particular non-monotonic finite-size corrections may still be important). It should also be noted that the weak-coupling analysis of Section 2.1 predicts a spin-gap. However, Figure 5 corresponds to a rather large value J'. In any case, according to our numerical data, a spin-gap seems to be at least very small if present at all. We have therefore not drawn an $\langle M\rangle = 0$ plateau (corresponding to a spin-gap) in Figure 5, though the speculative nature of the extrapolation in the region of small fields should be kept in mind.

For non-zero magnetizations, we use the following generalization of (4.2) as the criterion for a vanishing plateau width (compare also [63]):

$$h_{\mathrm{c}_2}(L) - h_{\mathrm{c}_1}(L) \sim \frac{1}{L}\cdot \tag{6.11}$$

At $\langle M\rangle = 2/3$ we find $h_{\mathrm{c}_2} - h_{\mathrm{c}_1} \approx 0.993J$, $0.584J$, $0.529J$ and $0.331J$ for $L = 4$, 6, 8 and 12, respectively. Although we cannot entirely rule out a tiny $\langle M\rangle = 2/3$ plateau on the basis of this data, it appears to be quite unlikely. We have therefore neither drawn a plateau at $\langle M\rangle = 2/3$ in Figure 5. In any case, our main result for PBC of type A is that one can observe a clear plateau with $\langle M\rangle = 1/3$.

6.2.2 Open boundary conditions

The limit $J \to 0$ of an N-leg zig-zag ladder with open boundary conditions gives rise to the recently introduced 'diagonal ladders' [64]. In particular, for $N = 3$ with open boundary conditions one recovers the necklace ladder at $J = 0$. This necklace ladder is very similar to the $S = (1, \frac{1}{2})$ ferrimagnetic chain which is known to exhibit a plateau with $\langle M\rangle = 1/3$ [65,66].

This strong-coupling limit $J \to 0$ suggests to choose L divisible by two, as does the weak-coupling limit $J' \to 0$. On the other hand, at $J' = J$ the $N = 3$ zig-zag ladder with open boundary conditions can be again considered as a strip of a triangular lattice which would suggest that L should be chosen a multiple of three. For the choice of parameters $J'/J = 3/2$ shown in Figure 6 divisibility by three turns out to be not important and we impose only divisibility by two.

The choice of parameters corresponding to Figure 6 ($\Delta = 1$, $J' = 3J/2$) appears to lie entirely in an incommensurate phase. At least at the transition $\langle M\rangle \to 1$, the momentum given by (6.6) is clearly incommensurate. The upper critical field is then found from (6.7) as $h_{\mathrm{uc}} = \frac{81}{16}J = 5.062\,5J$.

The finite-size magnetization curves in Figure 4 exhibit the expected plateau at $\langle M\rangle = 1/3$. In addition, there is clear evidence for a further plateau at $\langle M\rangle = 2/3$. The boundaries of these two plateaux were extrapolated applying either a Shanks transform (which is the $\alpha = 0$ special case of the vanden Broeck–Schwartz algorithm – see *e.g.* [67]) to their values $h_{\mathrm{c}_i}(L)$ at the available system sizes L, or (in the case of the upper boundary of the $\langle M\rangle = 1/3$ plateau) by fitting to

$$h_{\mathrm{c}_i}(L) = h_{\mathrm{c}_i}(\infty) + \frac{a}{L}\cdot \tag{6.12}$$

This heuristic formula is motivated by (6.11), since equation (6.12) can be expected to yield coincident plateau

boundaries if there is actually no plateau. In general, (6.12) will work well if it is applied to system sizes substantially below the correlation length and underestimate the width of a plateau otherwise. Here, it gives a small correction to the value for h_{c_i} obtained for the largest L, as does the Shanks extrapolation at the other plateau boundaries.

The finite-size spin-gap for $L = 4$, 6 and 8 is nicely fitted by (4.2). This indicates that there is no spin-gap at $h = 0$ and we have therefore not drawn an $\langle M \rangle = 0$ plateau in the extrapolated magnetization curve of Figure 6. Recently it was shown that a related three-leg ladder at zero field is also massless and gives rise to a $c = 2$ ($\widehat{su(2)}_2\times$ Ising) conformal field theory [68]. However there the chirally asymmetric perturbation was eliminated by a particular choice of coupling in order to permit an analytic treatment. In the present case the central charge might therefore be smaller than two.

The bold line in Figure 6 is an extrapolation taking into account the foregoing discussion of plateau boundaries. Between the plateaux it has been obtained by the same procedure as used in Figures 4 and 5.

6.2.3 PBC of type B and C

Inspection of the $r = 2$ version of (6.1) shows that at $J = 0$, the $N = 3$-leg zig-zag ladder with PBC of type B is equivalent to the $N = 2$-leg ladder with equal coupling constants. So, the results for the two-leg case discussed earlier can be carried over to this three-leg ladder at strong coupling. For example, this $N = 3$-leg ladder should exhibit incommensurate groundstate momenta at $J' \gg J$. More important for our purposes is that a small gap, but no other non-trivial plateaux are expected at strong coupling. To see to which extent this is generic, we show in Figure 7 numerical results obtained for the smaller value of $J' = 3J/2$. Figure 8 shows the analogous result for PBC of type C.

Since at $J = J'$, neither PBC of type B nor PBC of type C respect the sublattice structure of the triangular lattice, there is no reason to expect those L which are a multiple of three to play any particular rôle. We therefore simply consider even L.

If one ignores the bold extrapolated curves in Figures 7 and 8, the finite-size magnetization curves look quite similar at least if compared to the two boundary conditions discussed before. Such a similarity of PBC of type B and type C is also suggested by the fact that both of them can be mapped to a single chain (6.1). However, there are definitely at least quantitative differences, as already the value of the upper critical field shows: At $\Delta = 1$, $J'/J = 3/2$, one finds from (6.10) that $h_{\rm uc}/J = 5 + \frac{3}{8}\sqrt{3} \approx 5.6495$ for PBC of type B, while minimization of (6.8) with $r = 4$ yields $h_{\rm uc} \approx 6.1193J$ for PBC of type C.

The finite-size data for $L = 4$, 6 and 8 indicates a small spin-gap at zero field. For PBC of type B, application of a $1/L$-extrapolation in the spirit of (6.12) leads to a gap $\mathsf{E} \approx 0.24J$ while the Shanks transform yields $\mathsf{E} \approx 0.64J$. Though both methods agree on the presence of a gap, we are not able to determine it accurately – by comparison we conclude $\mathsf{E}/J = 0.44 \pm 0.20$ for PBC of type B. Similarly, for PBC of type C, the Shanks transform yields $\mathsf{E} \approx 0.27J$ while from (6.12) one finds $\mathsf{E} \approx 0.48J$. Here, we use the latter value though a large uncertainty should be kept in mind.

While one observes clear plateaux with $\langle M \rangle \neq 0$ in Figures 5 and 6, it is not immediately clear from the finite-size data of Figures 7 and 8 if such non-trivial plateaux survive the thermodynamic limit. This issue therefore requires a more detailed discussion. First we take a closer look at $\langle M \rangle = 1/3$. For PBC of type B, the finite-size plateau with $L = 4$, 6 and 8 is roughly (but not very well) fitted by (6.11). More strongly, one finds a negative plateau width if one tries to apply the extrapolation formula (6.12) to its boundaries. This indicates that there is not even a tiny plateau with $\langle M \rangle = 1/3$ in the thermodynamic limit $L \to \infty$. For PBC of type C in contrast, the plateau width at $L = 8$ is actually larger than that at $L = 6$. We have therefore drawn an $\langle M \rangle = 1/3$ plateau in Figure 8 whose boundaries have been determined using (6.12).

At $\langle M \rangle = 2/3$ we have data for a further system size ($L = 10$). If we discard the $L = 4$ data and ignore some apparent non-monotonic finite-size effects we actually obtain fairly good agreement with (6.11) in both cases. So, we do not find a plateau at $\langle M \rangle = 2/3$ in either of the two cases.

Extrapolated magnetization curves are shown by the bold lines in Figures 7 and 8. They have some remaining wiggly features which are related to the fact that non-monotonic finite-size effects may still be important at the system sizes used for the extrapolation.

The absence of a plateau *e.g.* at $\langle M \rangle = 1/3$ can be attributed to enhanced translational symmetry: The $N = 3$ zig-zag ladder with PBC of type B can be mapped to a single Heisenberg chain (6.1). A plateau at $\langle M \rangle = 1/3$ would then require breaking of the enhanced translational symmetry by $l = 3$ sites and a plateau at $\langle M \rangle = 2/3$ would require the even larger period of $l = 6$ sites (compare (1.1) where $V = l$ due to the enhanced symmetry). However, to the best of our knowledge spontaneous symmetry breaking with periods of more than two sites has not been observed so far (at least for ordinary ladders it is unlikely to occur [13]).

It should be mentioned though that the same argument can be applied to PBC of type C, where a plateau with $\langle M \rangle = 1/3$ seems likely. Furthermore, all versions of PBC are very similar from the weak-coupling point of view (compare Sect. 3). In particular, one would expect a plateau with $\langle M \rangle = 1/3$ for all versions of PBC if it appears for one of them in the weak-coupling region. Which plateaux are actually absent and which ones present therefore needs further investigation.

7 Discussion and conclusion

In this paper we have analyzed zig-zag coupled chains using a range of field-theoretical and numerical techniques.

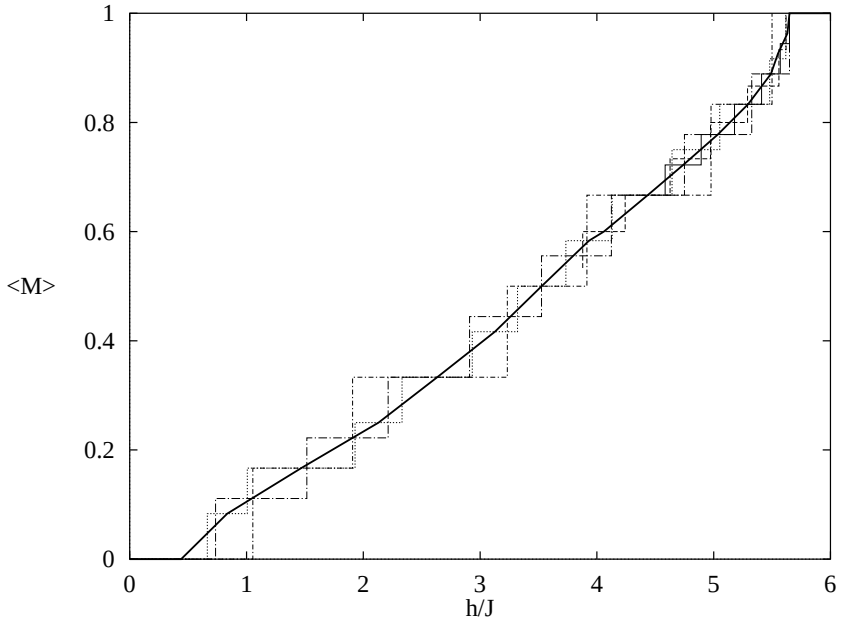

Fig. 7. Same as Figure 6, but for PBC of type B.

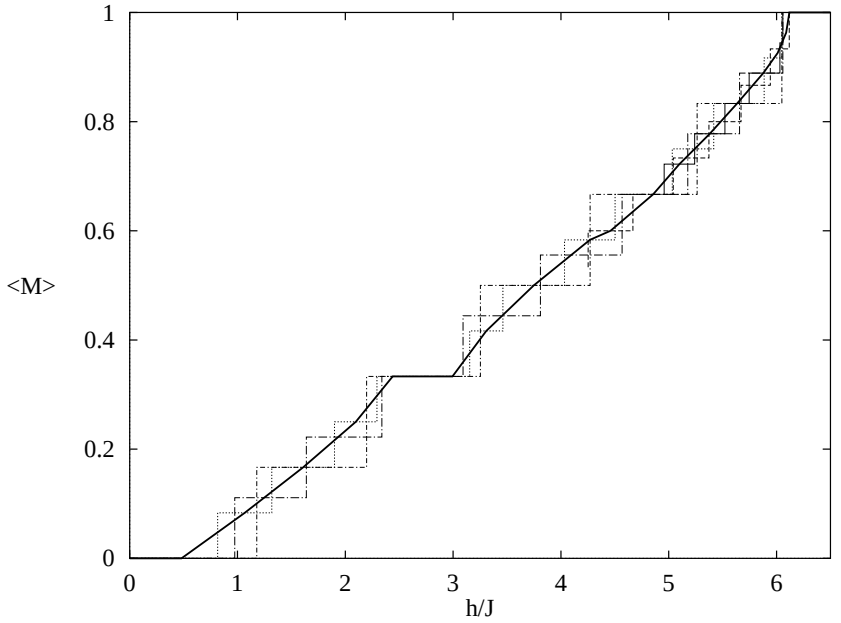

Fig. 8. Same as Figure 6, but for PBC of type C.

First, we have discussed the case of zero field and weak interchain coupling where in a field-theoretical formulation the most relevant interaction for the ordinary ladders is replaced with a chirally asymmetric one [24]. In the $SU(2)$ symmetric case this chirally asymmetric term is marginal and then current-current interaction terms (usually not considered in the presence of the relevant terms that arise in the normal ladders) have to be included in the RG analysis, leading us to our one-loop RG equations (2.10). In this approximation, one sees that the effect of the chirally asymmetric term is to push the system further into the massive phase for the AF case, and to open a gap for small $J' < 0$. The same is true for $N \geq 3$, when all the chains are (weakly) antiferromagnetically coupled in an equal manner. For sufficiently small $\Delta < 1$, the zero magnetization groundstate is a massless $c = 1$ theory, in contrast to the $N = 2$ ladder with normal couplings.

We have then shown that this more relevant interaction is restored by a magnetic field, dimerization or doping with charge carriers. The latter variants of zig-zag ladders

should therefore be similar to the usual spin ladders. We have also analyzed the appearance of plateaux in the magnetization curves of $N \geq 3$ zig-zag ladders. We have found that the situation is similar to that encountered in the normal ladders (in the weak coupling limit) [13], except for a trivial rescaling of the couplings which lead to slightly different quantitative predictions for the opening points.

These considerations may also be relevant to the description of experiments. Firstly, we have seen that under very general conditions the normal perpendicular couplings are those that really matter. Secondly, we have argued that dimerization along the legs (see Fig. 2) might be an important feature in understanding the magnetization experiments [28] on NH_4CuCl_3 (see also [20] for a related observation in the context of the usual spin ladders with dimerization along the chains). In the present context, this is suggested by the limit of strong dimerization $\delta \to 1$ which we have discussed in the appendix. Dimerization also seems to be a small enough modification to be plausible, but this will have to be confirmed by a determination of the structure of NH_4CuCl_3 at low temperatures.

The field-theoretical approach is complemented in a second part by a numerical analysis. First, we have analyzed a two-leg zig-zag ladder without dimerization. For positive J' we have confirmed known facts such as the appearance of a spin-gap but no non-trivial plateaux in the magnetization curve. The magnetized groundstates exhibit two different types of behaviour: At small J' incommensurate groundstate momenta participate in the magnetization process, while for small J all momenta are commensurate. For the case of ferromagnetic coupling $J' < 0$ we have found interesting new behaviour: At small $|J'|$ spins flip in pairs and for this reason all magnetized groundstates are commensurate. At larger $|J'|$ more than two spins can flip simultaneously and at the same time also incommensurate groundstate momenta become relevant to the magnetization process. Finally, for $J' < -4J$, the behaviour is completely ferromagnetic. The 'phases' with incommensurate groundstate momenta are reminiscent of similar phenomena observed in a spin-one chain [50,51]. It has been conjectured [50,53] that also the two-leg zig-zag ladder gives rise to a two-component Luttinger liquid, but at least in the weak-coupling region we did not find evidence for more than one massless degree of freedom.

We have then investigated the transition to saturation in more detail and confirmed the universal DN-PT behaviour (5.5). The only exception is $J' = 4J$ where a quartic behaviour (5.6) was already observed in [46]. This modified exponent has a simple explanation in terms of an exceptional behaviour of the single-spinwave dispersion which appears not to have been noted before. In the region of not too strong ferromagnetic $J' < 0$ spins flip in pairs and this relation to the single-spinwave dispersion is lost. It is therefore non-trivial that our numerical data for the asymptotics of the magnetization curve is still consistent with the DN-PT universal behaviour.

Finally, we have computed magnetization curves for four different variants of a three-leg ladder. We observed a remarkable dependence on the geometry of the interchain coupling (see Figs. 5–8). Clear plateaux can be observed in several cases while indications against the presence of such plateaux were obtained in other situations[3]. We expect that the same types of commensurate and incommensurate phases as observed for the two-leg ladder are also present in zig-zag ladders with three or more legs. This is indicated *e.g.* by the analysis of single-spinwave excitations for three-leg ladders, but would need verification. Further new phenomena might appear for more than two coupled chains.

All the observed plateaux can be interpreted in terms of the quantization condition (1.1). The essence is enhanced translational symmetry in certain cases which induced by frustration is then spontaneously broken (in most cases to periods $l \leq 2$). Specifically, for both the ordinary and the zig-zag two-leg ladder at $\delta = 0$ one then has a translationally invariant unit cell containing $V = 2$ spins. However, the interpretation is different: For zig-zag coupling, translational symmetry is first enhanced by a factor of two and then spontaneously broken by a period $l = 2$. This also explains why one needs a dimerized interchain coupling ($0 < \delta < 1$) to have a plateau with $\langle M \rangle = 1/2$ in the two-leg zig-zag ladder [12,39,40] which is permitted by (1.1) with $N = 2$, $l = 2$ only in the presence of dimerization. Dimerization along the legs breaks translational symmetry further to $V = 4l$. Frustration-induced spontaneous symmetry breaking to a period $l = 2$ then permits the aforementioned appearance of further plateaux with $\langle M \rangle = 1/4$ and $3/4$.

To interpret our results for the three-leg zig-zag ladders in terms of (1.1), one should substitute $V = 3l$ for OBC and PBC of type A and $V = l$ for PBC of type B and C. With one exception, all the plateaux sketched in Figures 5–8 can then be naturally interpreted with periods $l \leq 2$. Only the plateau with $\langle M \rangle = 1/3$ for PBC of type C in Figure 8 requires a period $l = 3$ which (if the presence of this plateau is confirmed) would be the highest observed period which we are aware of.

In fact, the numerical support for a plateau with $\langle M \rangle = 1/3$ for $N = 3$ and PBC of type C is rather weak and would deserve further attention. Conversely, the absence of a spin-gap in Figure 5 is not on safe grounds, and the Abelian bosonization analysis would actually predict at least a small spin-gap in the weak-coupling region. Another issue for $N = 2$ which requires further attention is that there is no numerical evidence yet for the spin-gap predicted by field theory for weak ferromagnetic $J' < 0$.

So far, we have just observed numerically for $N = 3$ that modifications in the boundary conditions have a drastic effect on the magnetization process. This is in

[3] It should be noted that due to non-monotonic finite-size effects it is difficult to reliably exclude plateaux not only in the cases discussed in Section 6 but also otherwise. Nevertheless, the evidence for or against a plateau *e.g.* at $\langle M \rangle = 1/3$ for $N = 3$ depends strongly on the boundary conditions.

contrast to ordinary spin ladders [13] and not apparent in the field theoretical treatment. It may be necessary to include higher loop corrections or to perform a non-perturbative analysis of the RG equations in order to understand how the novel interaction term arising from the zig-zag coupling gives for example rise to the differences in the different versions of PBC.

In summary, on the one hand we believe that we have exhibited interesting properties of zig-zag spin ladders. On the other hand, there is a number of points which deserve further attention. We hope that with this combination, the present paper will stimulate further research on zig-zag spin ladders.

We are indebted to A.A. Nersesyan for many useful discussions and a critical reading of the manuscript. We would also like to thank K. Le Hur, P. Lecheminant and M.E. Zhitomirsky for useful discussions and comments. D.C.C. would like to acknowledge financial support from CONICET, Fundación Antorchas, Deutsche Ausgleichbank, ANPCyT (under grant No. 03-00000-02249), the DAAD (under the Visiting Professors Programme) and thank the Physikalisches Institut der Universität Bonn for hospitality. The more involved numerical computations have been carried out on computers of the Max-Planck-Institut für Mathematik, Bonn-Beuel.

Appendix: Strong-coupling effective Hamiltonian for a dimerized two-leg ladder

In this appendix we consider the Hamiltonian for a two-leg zig-zag ladder with dimerized chains and coupling between the chains:

$$\begin{aligned} H = {} & J\sum_{i=1}^{2}\sum_{x=1}^{L}\big(1+(-1)^x\delta\big)\mathbf{S}_{i,x}\cdot\mathbf{S}_{i,x+1} \\ & + J'\sum_{x=1}^{L}\left\{(1+\delta')\mathbf{S}_{1,x}\cdot\mathbf{S}_{2,x}+(1-\delta')\mathbf{S}_{1,x}\cdot\mathbf{S}_{2,x+1}\right\} \\ & - h\sum_{i=1}^{2}\sum_{x=1}^{L}S^z_{i,x}. \end{aligned} \tag{A.1}$$

If we assume that $J'(1\pm\delta'), J(1-\delta) \ll J(1+\delta)$, we can describe the transition from $\langle M\rangle = 0$ to $\langle M\rangle = 1$ by an effective Hamiltonian following [3,12,16–19]. On each 'rung' (a bond coupled with coefficient $J(1+\delta)$) we retain only two states: The singlet and the fully polarized state. With an appropriate choice of basis, the first-order effective Hamiltonian can then be written as (note that we include the external magnetic field h in zeroth order):

$$\begin{aligned} H_{\text{eff.}} = {} & J(1-\delta)\sum_{x=1}^{L}\left\{\frac{1}{4}\left(S^+_xS^-_{x+2}+S^-_xS^+_{x+2}\right)+\frac{1}{4}S^z_xS^z_{x+2}\right\} \\ & + J'(1-\delta')\sum_{x=1}^{L/2}\left\{\frac{1}{4}\left(S^+_{2x}S^-_{2x+1}+S^-_{2x}S^+_{2x+1}\right)\right. \\ & \left.+\frac{1}{4}S^z_{2x}S^z_{2x+1}\right\} \\ & + J'(1+3\delta')\sum_{x=1}^{L/2}\frac{1}{4}\left(S^+_{2x+1}S^-_{2x+2}+S^-_{2x+1}S^+_{2x+2}\right) \\ & + J'(3+\delta')\sum_{x=1}^{L/2}\frac{1}{4}S^z_{2x+1}S^z_{2x+2} \\ & + \left(\frac{1}{4}J(1-\delta)+\frac{J'}{2}\right)\left(\frac{L}{4}+\sum_{x=1}^{L}S^z_x\right). \end{aligned} \tag{A.2}$$

The first term comes from one weak coupling $J(1-\delta)$ along the two original chains, the second one from one coupling $J'(1-\delta')$ between the two chains and the third and fourth terms arise from one coupling $J'(1-\delta')$ plus two couplings $J'(1+\delta')$ between the chains. The last term is just a first-order correction to the external magnetic field (apart from a trivial additive constant).

In equation (A.2) one recognizes again a two-leg zig-zag ladder with dimerized coupling between the chains. The coupling along the two chains is $J(1-\delta)$ with an effective XXZ anisotropy $\Delta_{\text{eff.}} = 1/2$. The coupling between the two chains is not only dimerized but also has an alternating XXZ anisotropy: $J'_{\text{eff.}} = J'(1-\delta')$, $\Delta'_{\text{eff.}} = 1/2$ on even sites, $J'_{\text{eff.}} = J'(1+3\delta')$, $\Delta'_{\text{eff.}} = (3+\delta')/(2(1+3\delta'))$ on the odd sites. For these values of parameters, the two-leg zig-zag ladder in a magnetic field has unfortunately not yet been studied in detail. However, this mapping is still suggestive since we know that a two-leg zig-zag ladder with dimerized coupling between the chains can exhibit plateaux at $\langle M_{\text{eff.}}\rangle = 0$ and $\langle M_{\text{eff.}}\rangle = \pm 1/2$ [12,39,40]. This suggests the possibility of the two-leg ladder with dimerized coupling along the chains (A.1) having not only plateaux at $\langle M\rangle = 0$ and $\langle M\rangle = 1/2$ (corresponding to $\langle M_{\text{eff.}}\rangle = 0$) but also at $\langle M\rangle = 1/4$ ($\langle M_{\text{eff.}}\rangle = -1/2$) and $\langle M\rangle = 3/4$ ($\langle M_{\text{eff.}}\rangle = 1/2$). This observation may be relevant to the magnetization experiments on NH_4CuCl_3 [28], since these are precisely the observed magnetization plateaux. However, in the strong dimerization limit considered in this appendix, one would certainly have a pronounced $\langle M\rangle = 0$ plateau which is not observed in NH_4CuCl_3. So, even if dimerization along the chains should be important in this compound, it cannot really lie in the region where the above mapping is applicable.

References

1. E. Dagotto, T.M. Rice, Science **271**, 618 (1996); T.M. Rice, Z. Phys. B **103**, 165 (1997).
2. B.G. Levi, Physics Today, October 1996, p. 17.
3. G. Chaboussant, M.-H. Julien, Y. Fagot-Revurat, M. Hanson, C. Berthier, L.P. Lévy, M. Horvatić, O. Piovesana, Eur. Phys. J. B **6**, 167 (1998).
4. K. Hida, J. Phys. Soc. Jap. **63**, 2359 (1994); K. Okamoto, Solid State Comm. **98**, 245 (1995).
5. T. Tonegawa, T. Nakao, M. Kaburagi, J. Phys. Soc. Jap. **65**, 3317 (1996).
6. M. Oshikawa, M. Yamanaka, I. Affleck, Phys. Rev. Lett. **78**, 1984 (1997).
7. G. Chaboussant, P.A. Crowell, L.P. Lévy, O. Piovesana, A. Madouri, D. Mailly, Phys. Rev. B **55**, 3046 (1997).
8. C.A. Hayward, D. Poilblanc, L.P. Lévy, Phys. Rev. B **54**, R12649 (1996).
9. K. Totsuka, Phys. Lett. A **228**, 103 (1997).
10. D.C. Cabra, A. Honecker, P. Pujol, Phys. Rev. Lett. **79**, 5126 (1997).
11. T. Sakai, M. Takahashi, Phys. Rev. B **57**, R3201 (1998).
12. K. Totsuka, Phys. Rev. B **57**, 3454 (1998).
13. D.C. Cabra, A. Honecker, P. Pujol, Phys. Rev. B **58**, 6241 (1998).
14. D.C. Cabra, M.D. Grynberg, Phys. Rev. B **59**, 119 (1999).
15. A. Honecker, Phys. Rev. B **59**, 6790 (1999).
16. F. Mila, Eur. Phys. J. B **6**, 201 (1998).
17. K. Tandon, S. Lal, S.K. Pati, S. Ramasesha, D. Sen, Phys. Rev. B **59**, 396 (1999).
18. K. Totsuka, Eur. Phys. J. B **5**, 705 (1998).
19. A. Furusaki, S.C. Zhang, Phys. Rev. B **60**, 1175 (1999).
20. D.C. Cabra, M.D. Grynberg, Phys. Rev. Lett. **82**, 1768 (1999).
21. R. Chitra, S.K. Pati, H.R. Krishnamurthy, D. Sen, S. Ramasesha, Phys. Rev. B **52**, 6581 (1995).
22. S.R. White, I. Affleck, Phys. Rev. B **54**, 9862 (1996).
23. D. Allen, D. Sénéchal, Phys. Rev. B **55**, 299 (1997).
24. A.A. Nersesyan, A.O. Gogolin, F.H.L. Eßler, Phys. Rev. Lett. **81**, 910 (1998).
25. E. Sørensen, I. Affleck, D. Augier, D. Poilblanc, Phys. Rev. B **58**, R14701 (1998).
26. R. Coldea, D.A. Tennant, R.A. Cowley, D.F. McMorrow, B. Dorner, Z. Tylczynski, J. Phys. Cond. Matter. **8**, 7473 (1996); Phys. Rev. Lett. **79**, 151 (1997).
27. W. Shiramura, K. Takatsu, H. Tanaka, K. Kamishima, M. Takahashi, H. Mitamura, T. Goto, J. Phys. Soc. Jap. **66**, 1900 (1997).
28. W. Shiramura *et al.*, J. Phys. Soc. Jap. **67**, 1548 (1998).
29. A.K. Kolezhuk, Phys. Rev. B **59**, 4181 (1999).
30. E. Altman, A. Auerbach, Phys. Rev. Lett. **81**, 4484 (1998).
31. S. Yunoki, J. Hu, A.L. Malvezzi, A. Moreo, N. Furukawa, E. Dagotto, Phys. Rev. Lett. **80**, 845 (1998).
32. C.K. Majumdar, D.K. Ghosh, J. Math. Phys. **10**, 1388 (1969); J. Math. Phys. **10**, 1399 (1969).
33. C.K. Majumdar, J. Phys. C: Solid State Phys. **3**, 911 (1970).
34. B.S. Shastry, B. Sutherland, Phys. Rev. Lett. **47**, 964 (1981).
35. E. Witten, Commun. Math. Phys. **92**, 455 (1984).
36. I. Affleck, in *Fields, Strings and Critical Phenomena, Les Houches, Session XLIX*, edited by E. Brézin, J. Zinn-Justin (North-Holland, Amsterdam, 1988).
37. T. Hikihara, A. Furusaki, Phys. Rev. B **58**, R583 (1998).
38. S. Lukyanov, A. Zamolodchikov, Nucl. Phys. B **493**, 571 (1997).
39. T. Tonegawa, T. Nishida, M. Kaburagi, Physica B **246-247**, 368 (1998).
40. A. Fledderjohann, C. Gerhardt, M. Karbach, K.-H. Mütter, R. Wießner, Phys. Rev. B **59**, 991 (1999).
41. D.G. Shelton, A.M. Tsvelik, Phys. Rev. B **53**, 14036 (1996).
42. H. Frahm, V.E. Korepin, Phys. Rev. B **42**, 10533 (1990).
43. T. Tonegawa, I. Harada, J. Phys. Soc. Jap. **56**, 2153 (1987).
44. T. Tonegawa, I. Harada, Physica B **155**, 379 (1989).
45. T. Tonegawa, I. Harada, J. Phys. Soc. Jap. **58**, 2902 (1989).
46. M. Schmidt, C. Gerhardt, K.-H. Mütter, M. Karbach, J. Phys. Cond. Matter **8**, 553 (1996).
47. C. Gerhardt, A. Fledderjohann, E. Aysal, K.-H. Mütter, J.F. Audet, H. Kröger, J. Phys. Cond. Matter **9**, 3435 (1997).
48. C. Gerhardt, K.-H. Mütter, H. Kröger, Phys. Rev. B **57**, 11504 (1998).
49. M. Usami, S. Suga, Phys. Lett. A **240**, 85 (1998).
50. G. Fáth, P.B. Littlewood, Phys. Rev. B **58**, R14709 (1998).
51. O. Golinelli, Th. Jolicoeur, E.S. Sørensen, Eur. Phys. J. B **11**, 199 (1999).
52. R.J. Bursill, G.A. Gehring, D.J.J. Farnell, J.B. Parkinson, T. Xiang, C. Zeng, J. Phys. Cond. Matter **7**, 8605 (1995).
53. H. Frahm, C. Rödenbeck, Eur. Phys. J. B **10**, 409 (1999).
54. T. Hamada, J. Kane, S. Nakagawa, Y. Natsume, J. Phys. Soc. Jap. **57**, 1891 (1988).
55. J.C. Bonner, M.E. Fisher, Phys Rev. **135**, A640 (1964).
56. J.L. Cardy, J. Phys. A **17**, L385 (1984).
57. R.P. Hodgson, J.B. Parkinson, J. Phys. C **18**, 6385 (1985).
58. G.I. Dzhaparidze, A.A. Nersesyan, JETP Lett. **27**, 334 (1978).
59. V.L. Pokrovsky, A.L. Talapov, Phys. Rev. Lett. **42**, 65 (1979).
60. H. Nishimori, S. Miyashita, J. Phys. Soc. Jap. **55**, 4448 (1986).
61. A. Honecker, J. Phys. Cond. Matter **11**, 4697 (1999).
62. K. Kawano, M. Takahashi, J. Phys. Soc. Jap. **66**, 4001 (1997).
63. T. Sakai, M. Takahashi, Phys. Rev. B **43**, 13383 (1991); J. Phys. Soc. Jap. **60**, 3615 (1991).
64. G. Sierra, M.A. Martín-Delgado, S.R. White, D.J. Scalapino, J. Dukelsky, Phys. Rev. B **59**, 7973 (1999).
65. T. Kuramoto, J. Phys. Soc. Jap. **67**, 1762 (1998).
66. K. Maisinger, U. Schollwöck, S. Brehmer, H.-J. Mikeska, S. Yamamoto, Phys. Rev. B **58**, R5908 (1998).
67. M. Henkel, G.M. Schütz, J. Phys. A **21**, 2617 (1988).
68. P. Azaria, P. Lecheminant, A.A. Nersesyan, Phys. Rev. B **58**, R8881 (1998).